Chapter 12

# Recent Advances in Wavelength-Division-Multiplexing Plastic Optical Fiber Technologies

David Sánchez Montero, Isabel Pérez Garcilópez,
Carmen Vázquez García, Pedro Contreras Lallana,
Alberto Tapetado Moraleda and
Plinio Jesús Pinzón Castillo

Additional information is available at the end of the chapter

http://dx.doi.org/10.5772/59518

## 1. Introduction

Growing research interests are focused on the high-speed telecommunications and data communications networks with increasing demand for accessing even from the home, due to the huge successes during the last decade of new multimedia services (high-definition (HD), three-dimensional visual information (3D) or remote "face-to-face communication") which forecast requirements for data transmission speed more than 40Gbps by 2020, which can be achievable only with optical network [1]. Regarding this data transmission capability, Polymer Optical Fiber (POF) technology has emerged as a useful medium for short-reach distances scenarios such as Local Area Networks (LANs), in-home and office networks, automotive and avionic multimedia buses or data center connections among others. However, its potential capacity for communication needs a greater exploitation to meet user requirements for higher-data rates.

The strong increase of bandwidth demand presents an increasing challenge for service operators to delivery their high-quality service to the end user's device. At this moment, commercially available progressive service plans range between the 50-100Mbps while premium services typically range around 100-150Mbps. And it should be reminded that the bandwidth in the local loop is forecasted to grow with an average of 20-50% annually. Recent interests are focused on gigabit-order data transmission, being desirable, at the same time, to introduce optical fiber networks even to the customer´s premises for covering more than 10Gbps in the near future, introducing the concept of FTTx (Fiber To The Home/Node/

Building/Curb) deployments. There is a worldwide consensus that the optical fiber solution provides enough bandwidth to attend user's demand at the required transmission distances in the short-reach domain (typically up to 200m).

In this optical fiber network deployment scenario, POF offers several advantages over conventional silica multimode optical fiber over short distances. Such fiber type can provide an effective solution as its great advantage is the even potential lower cost associated with its easiness of installation, splicing and connecting. This is due to the fact that POF have higher dimensions, larger numerical aperture (NA) and larger critical curvature radius in comparison with glass optical fibers [2]. Moreover, it is more flexible and ductile, making it easier to handle. Consequently, POF termination can be realized not only faster but also cheaper than in the case of multimode silica optical fiber [3]. To summarize, POFs have multiple applications in sensor systems at low or competitive cost compared to the well–established conventional technologies [4].

To date, most used POF type is the step index POF (SI-POF) but many variants have been manufactured and tested showing different performances between them [5]. SI-POF is made of polymethyl-methacrylate (PMMA), (also called standard POF) and it has 980 μm core diameter, 10 μm cladding thickness and 0.5 NA. However, SI-POF suffers from high modal dispersion, which reduces the usable bandwidth to typically 50 MHz × 100 m [6]. And it is only used in the visible spectrum range (VIS), where it can provide acceptable attenuation (e.g. 100 dB/Km at 650 nm) [5]. This is because of the large attenuation due to the high harmonic absorption loss by carbon-hydrogen (C-H) vibration (C-H overtone). However, improvements in the bandwidth of POF fiber can be obtained by grading the refractive index, thus introducing the so-called Graded-Index POFs (GIPOFs). Although firstly developed PMMA-GIPOFs were demonstrated to obtain very high transmission bandwidth compared to that of SI counterparts [7], the use of PMMA is not still attractive due to its strong absorption at the near-infrared (near-IR) to infrared (IR) regions. As a result, PMMA-based GIPOFs can only be used at a few wavelengths in the visible portion of the spectrum. Today, unfortunately, almost all gigabit optical sources operate in the near-infrared (typically 850nm or 1300nm), where PMMA and similar polymers are essentially opaque. Reduction of loss has been achieved by using amorphous perfluorinated polymers for the core material. This new type of POF has been named perfluorinated GIPOF (PF GIPOF), and has a relative low loss wavelength region ranging from 650nm to 1300nm (even theoretically in the third transmission window) [8]. Consequently, available off-the-shelf light sources for silica fiber based systems can be used with PF-GIPOF systems. In 1998, the PF-based GIPOF had an attenuation of around 30dB/km at 1310nm. Attenuation around 20dB/km was achieved only three years after and lower and lower values of attenuation are being achieved. The theoretical limit of PF-based GIPOFs is ~0.5 dB/km at 1250-1390nm [9]. Nevertheless, although these losses are coming down steadily due to ongoing improvements in the production processes of this still young technology, the higher than silica attenuation inhibits their use in relative long link applications, being mainly driven for covering in-building optical networks link lengths for in-building/home optical networks (with link lengths less than 1 km), and thus the loss per unit length is of less importance. In addition, PF-GIPOF can provide a bandwidth per length product ~400MHz x

http://dx.doi.org/10.5772/59518

km at both 850nm and 1300nm, respectively, and can support bit rates of 40Gbps up to 200m for any launch condition [10]. This fact is due to the PF-GIPOF low material dispersion characteristics (even lower compared to silica multimode optical fibers) [11].

Although POFs reveal a cost effective solution for short-reach optical deployments, their bandwidth characteristics still limit the reach distances and the capacity to attend future end users' transmission requirements. These facts hamper the desired integration of multiple broadband services into a common multimode fiber access or in-building/home network. Overcoming the bandwidth limitation of such fibers requires the development of techniques oriented to extend the capabilities of POF networks to attend the consumer's demand for multimedia services. Different efficient and advanced modulation formats and/or adaptive electrical equalization schemes can alternatively be applied. Considering the industry's extensive experience and the large economies of scale, orthogonal frequency division multiplexing (OFDM) [12], subcarrier multiplexing (SCM) [13] and discrete multitone modulation (DMT) [14] are seen as promising technologies for low-cost, reliable, and robust Gigabit transmission through hundreds of meters of POF. Particularly, DMT modulation has been demonstrated to achieve near-optimum performance and to enable highly spectral efficient transmission at high bit-rates over silica multimode fibers (MMFs) and POFs [15, 16]. Initially, transmission with SI–POF has been realized with only one channel, typically at 650 nm, reaching data rates of 100 Mb/s over links of 275 m [17]; even multi−gigabit transmission over links of 50 m has been reached [18]. Commercial systems with data rates of 1 Gbit/s via up to 50 m of SI−POF with a single channel have also been reported [19]. Moreover, theoretical simulations with data rates of 1.25 Gbit/s, 2.1 Gbit/s [20] and 6.2 Gbit/s [21], via up to 50 m of SI-POF using a single channel with NRZ, CAP-64 and QAM512 modulations, respectively, have been demonstrated.

After exploiting the capabilities of a single channel, the next step to increase the capacity of an individual POF is to use multiple channels over a single fiber what is well known as wavelength division multiplexing (WDM). In the last years, WDM techniques over POFs are being proposed to expand the usable bandwidth of POF-based systems. For instance, Jončić *et al.* [22] firstly reported a 10 Gbit/s transmission over 25 m of SI−POF using offline-processed NRZ modulation. Beyond that, same authors achieved data rates up to 14.77 Gbit/s, with 4 channels via up to 50 m of a SI−POF link using offline-processed discrete multitone modulation [23]. In the same way, many POF based sensors implement self–referencing schemes by transmitting different wavelengths over a single fiber [4]. However, there are some constrains that must be addressed in order to perform the same capabilities as in the case of silica-based WDM approaches. In the WDM technique, different wavelengths which are jointly transmitted over the fiber must be separated to regain all information. Therefore, for a typical WDM optical communication link two key-elements are, at the very least, indispensable and have to be introduced, a multiplexer and a demultiplexer. The former is placed before the single fiber to integrate every wavelength to a single waveguide. The latter is placed behind the fiber lead to regain every discrete wavelength. These two components have long been established for silica-based infrared telecom systems, bust must be developed completely new for POF-based WDM applications. The most common and grave disadvantage almost all of these approaches exhibit

is their costly production, which makes them unsuitable for today's price sensitive mass markets. The underlying reason behind this lack of development is the mismatch between the optimum operating wavelength regions of POFs and the optical devices exploited for telecommunications purposes. The latter are developed for a wavelength region (C- and L-bands) totally unsuitable for POF-based transmission over medium-distances (hundreds of meters or greater) due to the high attenuation of PMMA based POF of around 1dB/cm@1550nm. A similar conclusion can be obtained for PF-GIPOFs which attenuation characteristics are not at par with that of standard silica based fibers, but still superior to that of copper based technologies and PMMA-POF fibers. Another question to be addressed is the large POF dimensions and NA, which produce beams with high divergence thus being difficult to be routed. In addition, multiplexed systems operating in VIS range for POF networks may need reconfiguration because they do not have standard channels as well as provide flexibility in the networks to be developed.

In this framework, this chapter is intended to be a progress report and it will focus on the state-of-the art, description and experimental validation of different POF-based key devices that provide an easy-reconfigurable performance for WDM applications. Novel multiplexers/demultiplexers, variable optical attenuators, interleavers, switches and optical filters to separate and to route the different transmitted wavelengths are described. The main target is to bridge the gap of the WDM POF-based network deployment bottleneck in the final leg of delivering. In addition, a hybrid silica-POF WDM-PON network is analyzed showing the capabilities of novel Fiber Bragg Gratings (FBG) inscribed on microestructured POF devices to be compatible with WDM topologies for both sensing and communication schemes. Moreover, the theoretical capacity for a future WDM-GIPOF deployment is addressed taking advantage of the performance of this recent fiber type. Finally the main conclusions are presented.

## 2. Optical multiplexers and demultiplexers in POF technology

Multiplexers, combiners and variable optical attenuators are basic elements in POF networks when using the WDM approach but are not widely spread yet on the market due to the aforementioned reasons yielding their associated insertion losses. Nevertheless, reconfiguration can be an additional feature for those networks but most of them developed in POF technology do not provide such a characteristic. In this section, novel POF devices with reconfigurable characteristics for WDM applications addressing compact, scalable and low consumption solutions and with low insertion losses will be described. They operate at the wavelengths of interest for POF applications and their performance will be compared to current state-of-the-art approaches reported in literature. Some of them will take advantage of the properties of liquid crystal materials.

Several technologies have been reported for implementing optical multiplexers. Arrayed Waveguides Gratings (AWG), based on two multimode interference sections joined through several waveguides of different lengths, are proposed to be used in short distance communi-

http://dx.doi.org/10.5772/59518

cations [24]. However, this approach is unsuitable for the wavelength range of operation of POF networks with affordable losses and, therefore, cannot be used. On the other hand, in the WDM approach many transmitters with different light colors can carry individual information. In WDM-POF systems, most multiplexers used in POF links are based on N:1 splitting devices which their function is to combine the optical signals from multiple different single-wavelength end devices at their inputs onto a single output fiber. For example, red light can be modulated with Ethernet data while blue, green and yellow light can carry image information, radio frequency (RF) and television signal, respectively. There have been many techniques of fabricating POF couplers. These techniques include twisting and fusion, side polishing, chemical etching, cutting and gluing, thermal deformation, molding, biconical body and reflective body [25]. The main drawback of the use of POF couplers as multiplexers are: a) their high associated insertion losses, typically up to 8dB per branch [26] if we consider 3:1 and 4:1 POF couplers; and b) in this kind of multiplexers input ports are not interchangeable and each input port must be excited by a pre-allocated wavelength source. To solve this latter disadvantage, another approaches make use of novel reconfigurable POF multiplexing devices, where inputs are wavelength independent, as they work in the same way for different wavelengths, thus allowing more flexibility in WDM-POF networks. They will be described in the following section.

From the POF demultiplexer perspective, solutions for WDM SI-POF networks reported in literature are based on bulk optics and take advantage of discrete devices such as prisms [27], thin-film filters [28] or diffraction gratings [29, 30]. Thin-film based demultiplexers are easy to implement and are a good choice to design demuxes with low insertion loss and multiple channels. However, they are large, require many elements (typically the number of elements doubles the number of channels) and their channel isolation (crosstalk) is mainly limited by the rejection ratio of the thin-film filters used. Optical filtering at each output channel is usually employed to enhance the crosstalk performance in this type of demultiplexers thus adding complexity into the system. In contrast, prism-based demultiplexers have few elements and are cheaper but usually show a low performance in terms of both insertion loss and crosstalk. Most common proposals are based on concave gratings. These proposals have good expectations as they have a small size and because the light spatial separation and its focusing are performed with a single element. However, they require diffractive elements that to date are not easy to manufacture and have not reached large market volumes yet, being a costly solution. Moreover their experimental performance has not yet been tested on a mass basis real scenario. However, it is expected to experience the price reductions accompanying economy-of-scale in a near future.

### 2.1. Designs of reconfigurable optical multiplexers

Among the different technologies used for implementing optical multiplexers (as well as for optical switches) those based on liquid crystals (LC) are very interesting because they do not have mobile parts, need low excitation voltages and have a low power consumption. In the last years, liquid crystal has been widely used in displays applications. Liquid crystals are organic compounds that have properties intermediates between liquid and crystalline solids

[31]. They have anisotropic characteristics such as the dielectric constant or the refractive index, like solids, but simultaneously they are fluids. There are mainly two types of LC used in optical multiplexing, Ferroelectric Liquid Crystals (FLC) [32] and Nematic Liquid Crystal (NLC) [33-35], both normally using the structure of a Twisted Nematic Liquid Crystal cell (TN-LC). The first ones have a better response time but they can operate in a smaller wavelength range. The second ones have worst response times (tens of milliseconds in conventional mixtures), but they can operate in a wider wavelength range because they only have to fulfill Mauguin's regime $\Delta n \; x \; d/\lambda >> 1$ in order to obtain the polarization shift, where $\Delta n$ is the birefringence of the LC, $d$ the LC cell thickness and $\lambda$ the wavelength, respectively.

In the following, different topologies of optical multiplexers based on liquid crystals are described. The first design is based on Polymer Dispersed Liquid Crystal (PDLC), which is a special case of NLC, while the other devices are based on TN-LC cells. A brief introduction about both LC types is provided within each section for a better understanding.

### *2.1.1. Optical multiplexer and variable optical attenuator based on polymer dispersed liquid crystal*

The first design of the proposed multiplexers is based on PDLC. PDLC is composed by microdroplets with liquid crystal molecules dispersed in a polymeric matrix. Liquid Crystal molecules have electrical and optical birefringence, which means that the molecules have different dielectric constants and refractive indexes depending on the molecule axes. This mixture is sandwiched between glasses and covered with a transparent conductor [36]. In this way, an electric field can be applied to the mixture allowing the reorientation of the liquid crystal molecules that are inside the microdroplets thanks to the molecule birefringence. The structure of the PDLC cell is shown in Fig. 1.

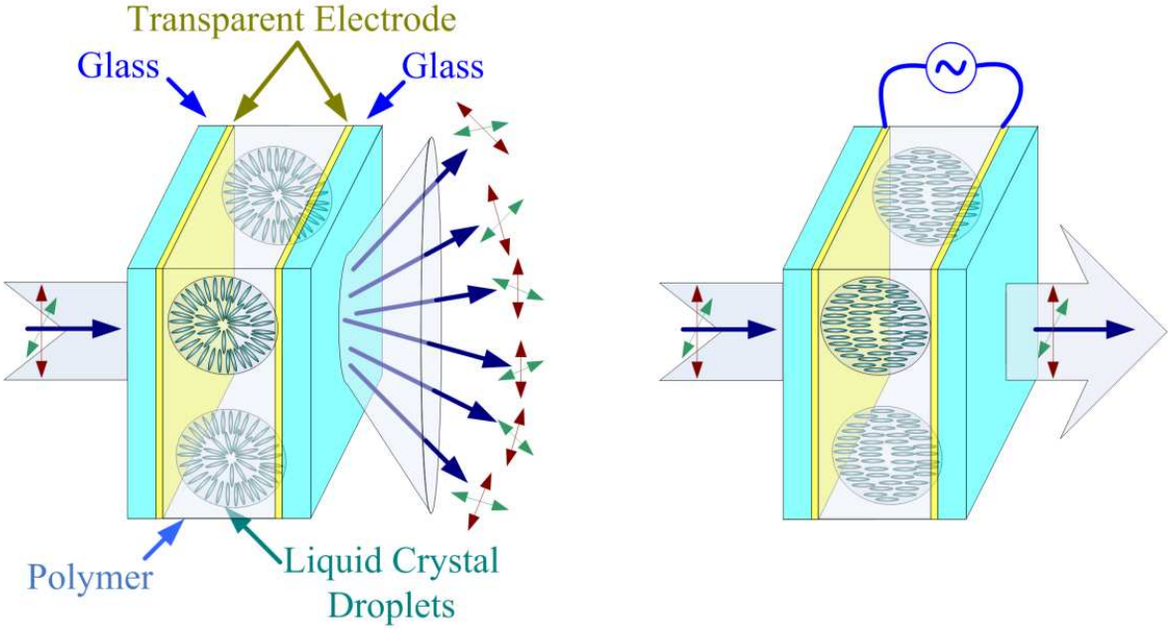


**Figure 1.** Structure of a Polymer Dispersed Liquid Crystal cell

http://dx.doi.org/10.5772/59518

The principle of operation is the following. At resting state, i.e. there is no voltage applied to the transparent conductors (electrodes), the liquid crystal molecules inside the droplets do not have a predominant orientation and the light that passes through the mixture find different refractive indexes. Therefore, it is highly scattered into different directions. On the other hand, if enough voltage is applied between the transparent conductors, an electric field is created inside the mixture and the liquid crystal molecules are forced to follow the induced electric field. In this case, the mixture has a homogeneous refractive index and the light that passes through the mixture is not refracted and maintains the same propagation direction. In addition to this, there is a gradual transition in the liquid crystal molecules reorientation, thus, if the voltage applied is not high enough, the molecules are not fully oriented but the light that passes through the mixture is less scattered [37].

Due to the possibility for controlling the transmission of light through the PDLC, the latter have been mainly reported for implementing Variable Optical Attenuators (VOA) [38, 39]. A VOA based on a 2 x 2 coupler made of POF is presented in [38]. The idea for implementing a reconfigurable optical multiplexer based on PDLC is to use the PDLC cell with several pixels as the active element [40]. The structure is shown in Fig. 2. The input ports, that are optical fibers, are placed in front of each pixel of the PDLC cell. The light that comes out from the fiber is spreaded according to the numerical aperture of the optical fiber, thus, the lenses placed in front of each input port are required for collimating the light that comes out from the optical fibers. The light from each input port passes through one pixel of the PDLC cell and finally, the lens placed at the output focuses the light into the output fiber.

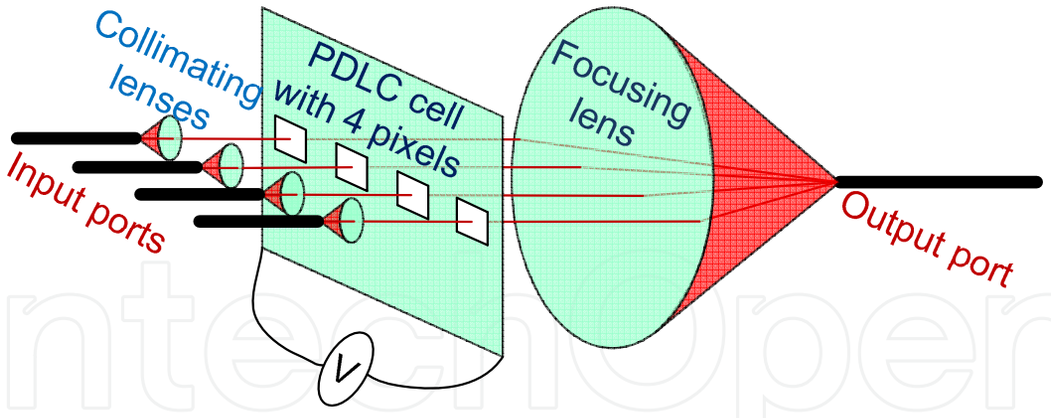


**Figure 2.** Structure of the reconfigurable optical multiplexer based on PDLC

By using the proposed structure, when no voltage is applied to the PDLC pixel, the light that comes from the input port is scattered in the PDLC cell and, therefore, it is not focused in the output port. On the contrary, when enough voltage is applied to the PDLC cell, the light can pass through the PDLC cell being focused on the output port. In addition, variable attenuation can be achieved by applying intermediates voltages. Each pixel can be addressed independently from the adjacent ones, so each input port can be switched on/off without affecting the others.

The introduced reconfigurable optical multiplexer can also acts as a variable optical attenuator. It can operate in the visible range as POF do. The typical voltage value for switching the PDLC is tenths of volts. The achieved insertion loss is about 1.6dB, the crosstalk obtained is in the range of 30dB, and finally, the response time of the PDLC is in the order of tenths of milliseconds.

*2.1.2. Optical multiplexers based on Twisted Nematic Liquid Crystals (TN-LC)*

Other way in which liquid crystal is used is known as TN-LC. In this kind of devices, the liquid crystal is also sandwiched between two glasses covered with a transparent conductor (electrode). However, the glasses have an additional rubbed alignment film that forces the LC molecules to have an orientation. In a TN-LC the orientation of the LC molecules in one glass is perpendicular to the molecular orientation in the other glass. Thanks to these constraints, the LC molecules inside the cell perform a helix from one glass to the other. The structure of a TN-LC cell is shown in Fig. 3.

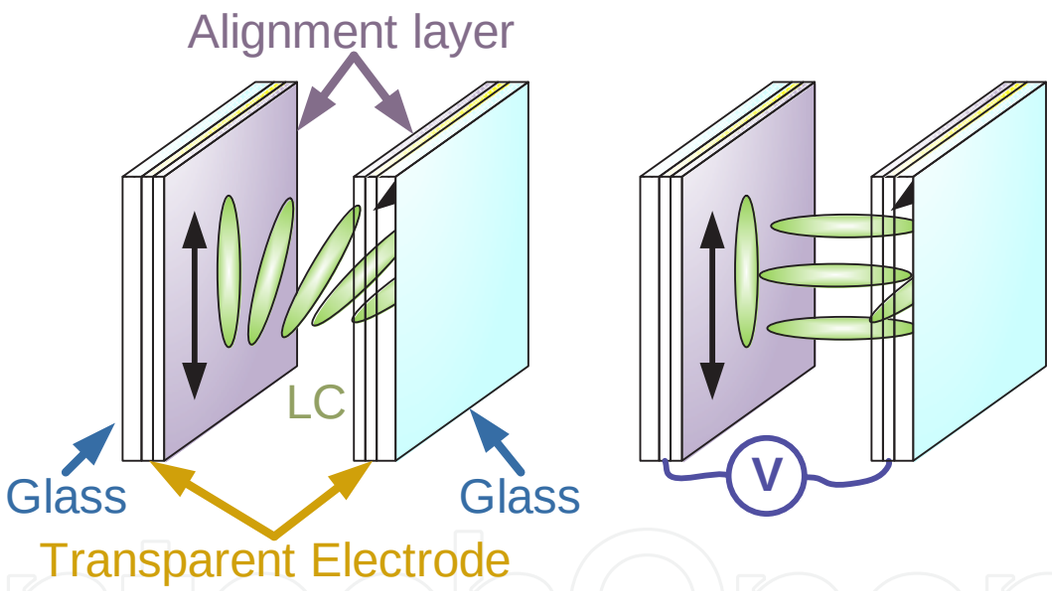


**Figure 3.** Structure of a twisted nematic liquid crystal cell.

The principle of operation is the following. If no voltage is applied to the LC, the polarization of the light that passes through the TN-LC cell is ideally rotated 90 degrees. On the other hand, when enough voltage is applied between the transparent conductors of each glass, an electric field is generated inside the cell, and the molecules are reoriented to be perpendicular to the glasses. In this scenario, the polarization of the incident light remains when passes through the LC.

In this way, the polarization of the light that transverse the TN-LC cell can be controlled. Thus, by placing the TN-LC cell between polarizers, the transmission of the incident light can be modified by means of the voltage applied to the cell. A polarizer placed before the TN-LC cell

http://dx.doi.org/10.5772/59518

allows passing only one polarization of the incident light. In this way, a polarized light beam enters in the TN-LC cell. The TN-LC controls its polarization stage depending on the voltage applied to the cell. Finally, the polarizer placed after the TN-LC filters, or not, the light that comes out from the TN-LC cell. According to the TN-LC operation, there are two ways of implementing the device for controlling the light transmission: a) putting the TN-LC cell between crossed polarizers, or b) putting it between parallel polarizers. In the first case, the light passes through the device when there is no voltage applied to TN-LC while light is stopped when enough voltage is applied to the LC cell. On the contrary, the input light is blocked by the device when no voltage is applied to the TN-LC cell and the light passes through the device when enough voltage is applied to the TN-LC cell. The procedure described has been mainly used in displays applications [41], but it can also been used for optical multiplexing as well as for optical switching. The latter will be seen in a following section.

As previously reported, multiplexers and demultiplexers are basic elements in those optical networks where WDM is implemented because they combine different wavelengths in a single fiber. POF fiber has a low attenuation in the visible wavelength region (at 450nm, 550nm and 650nm), for this reason, the optical multiplexers must work in this wavelength range. An example of a reconfigurable multiplexer based on TN-LC cells is presented in Fig. 4 [42]. The introduced structure of the multiplexer can be used in several wavelength ranges depending on the bulk elements used.

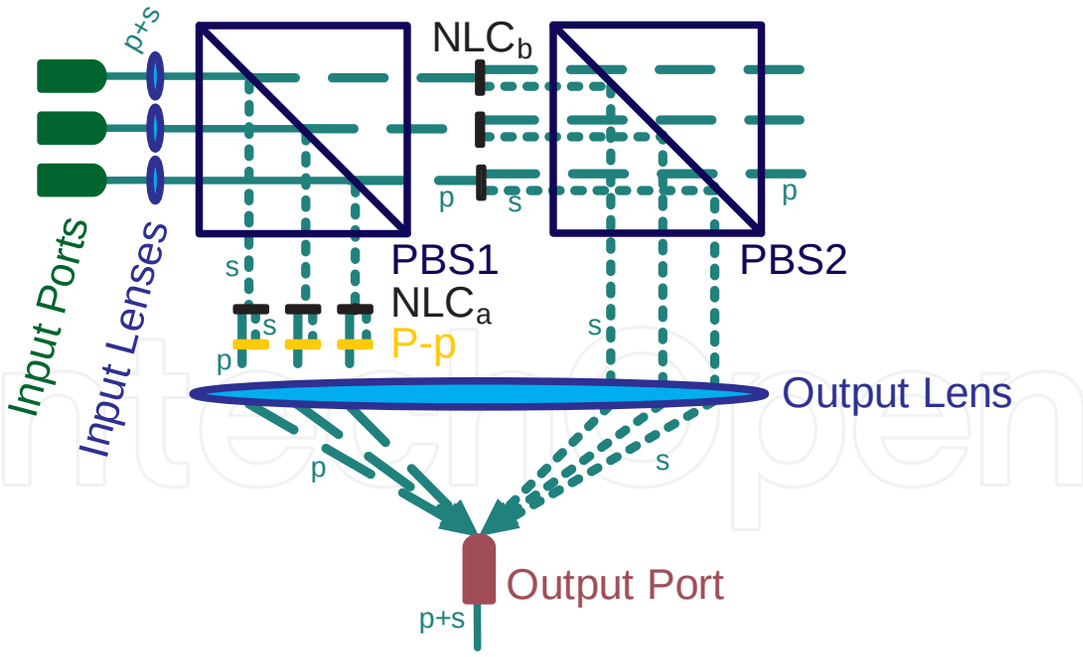


**Figure 4.** Structure of the reconfigurable 3x1 optical multiplexer.

The structure is composed by Polarizing Beam Splitters (PBS1 and PBS2), TN-LC cells (NLCa and NLCb), polarizers and lenses. There are three input ports, and a single output port. Each TN-LC cell has three pixels, and each pixel controls the transmission of one input port.

Consequently each input port can be managed independently of the others. The input lenses are required for collimating the light that comes from each input fiber, and the output lens focuses each beam into the output port.

The operation of the optical multiplexer makes that the light from one input port is guided to the output port when there is no voltage applied to the corresponding pair of pixels of liquid crystal cells. If a voltage is applied to theses pixels, the light from the input port is not guided to the output port.

*2.1.3. Advanced multifunctional optical multiplexer for multimode optical fiber networks*

In passive optical networks where there is no additional amplification, it is important to have few insertion losses. It could be also interesting to have additional functions in the same device and thus reducing the number of devices in the optical network. In addition to that, reconfigurable optical networks in critical applications where an alternative path is required when there is a failure in the main path would be useful.

An improvement in terms of flexibility of the 3x1 multiplexer shown in the above figure is presented in Fig. 5 [43]. The structure has two set of three inputs and two outputs, and depending on the configuration each input of the one set of inputs can be guided to one of the two possible outputs.

The structure can implement different functionalities only by selecting the inputs, the outputs and modifying the voltage applied to the TN-LC pixels of each cell. It can behave as a 3x1 multiplexer (or combiner) using only three inputs and one of the outputs, each input port can be switched on/off independently of the other three inputs thus also acting as an optical switch if required.

The same device can operate as two complementary 3x1 Multiplexers. Inputs to the device are grouped in pairs, when the *Input Port a* is guided to *Output Port 1*, the other input of this pair, *Input Port b*, is coupled to *Output Port 2*. On the other hand, when the multiplexer is switched, *Input Port a* is directed to *Output Port 2* and the matched *Input Port b* is propagated to *Output Port 1*. As a matter of fact, it can also work as a 2x2 optical switch by using only the adequate pair of inputs and the two outputs.

The use of TN-LC cells allows having intermediate values of light transmission by applying lower voltage, so the device can also implement a VOA by using a single input port and only one of its outputs. Finally, it can also implement a variable optical power splitter by using one input and its two outputs.

The introduced reconfigurable Advanced Multifunctional Optical Multiplexer has fiber to fiber insertion losses when operating as a 2x2 optical switch, in the range from 10dB to 15dB within 200nm wavelength range; with a non-optimized optics for collimation and coupling. Lower losses can be achieved for a smaller wavelength range. The crosstalk measured is better than -15dB at 532nm, 660nm and 850nm. Switching is achieved at voltage levels of $4V_{RMS}$.

http://dx.doi.org/10.5772/59518

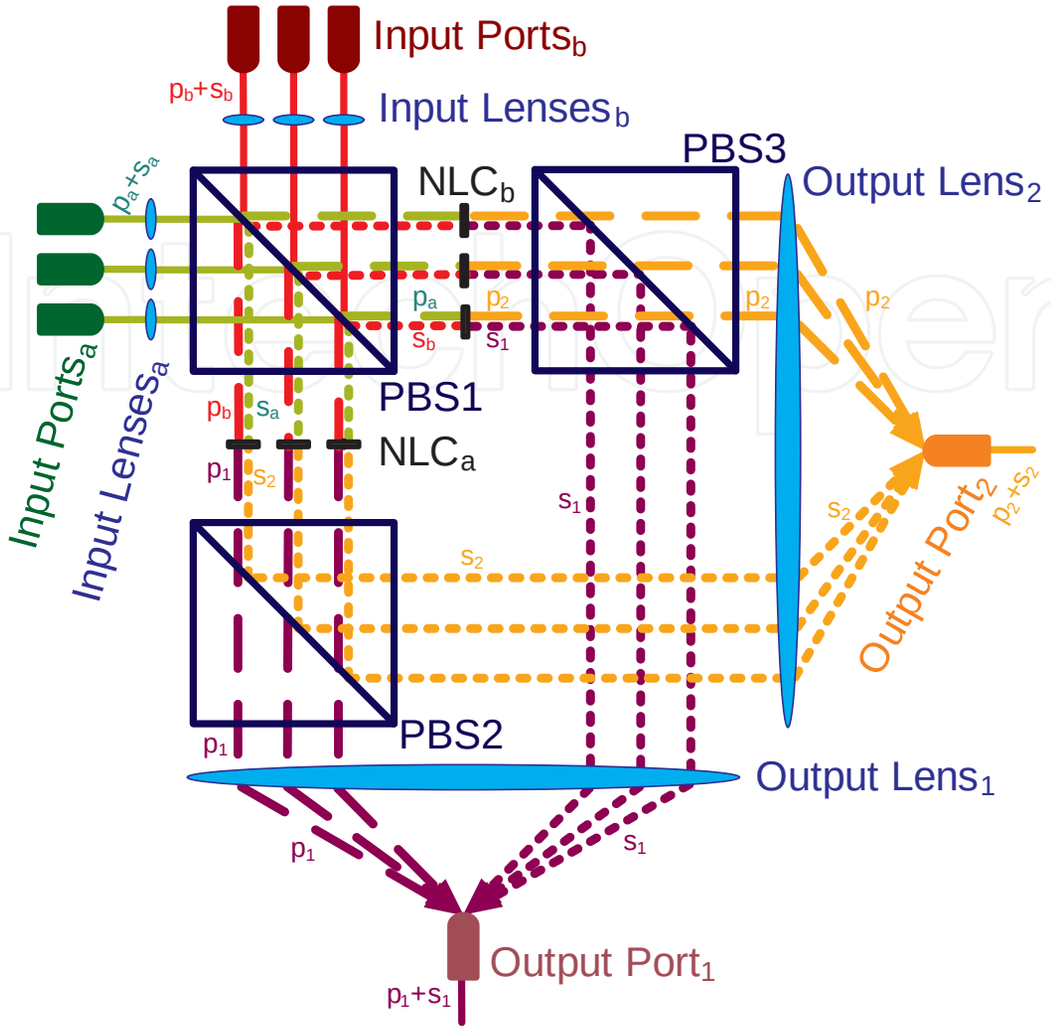


**Figure 5.** Structure of the Advanced Multifunctional Optical Multiplexer. It design also allows switching functionality if required into a single device.

## 3. Optical routing for WDM POF-based applications

For WDM routing, key devices such as interleavers, routers and switches are also indispensable to combine, to separate and to re-direct the different transmitted wavelengths. Nowadays, WDM devices are well-established in the IR and near IR (NIR) for silica optical fibers. However, they require a complete re–design for being implemented in SI–POF WDM systems. This is mainly due to their distinct attenuation behavior (compared to silica fiber) and new wavelength channels need to be determined. Nevertheless, there is no a widely spread consensus about the characteristics for these WDM channels for POF applications, although some authors have already proposed a spectral grid [44], which includes channels between 400 nm and 700 nm and spectral bandwidths up to 50 nm (LED sources) [45].

Nowadays, optical routers are key components in optical communications and sensor networks. Optical switches allow optical routing without converting the transmitted infor-

mation into the electrical domain. The elimination of the two required conversions (optical to electrical and electrical to optical) improves the system characteristics, reducing the network equipment and increasing their bandwidth. These devices work by selectively switching optical signals delivered through one or more input ports to one or more output ports, in response to supervisory control signals. Different technologies could be applied to route optical signals, applications of which depend on the topology of the optical network and the switching speed required [46]. Cutting-edge optical switching technologies depending on their principle of operation include micro-electromechanical systems (MEMS) as well as acousto-optical, thermo-optical, opto-optical and electro-optical (EO) devices.

Opto-Mechanical switches are based on the movement of some mechanical devices such as prisms, mirrors or directional couplers. As a subsection of the opto-mechanical technology, MEMS have a great interest in telecommunications applications. MEMS consist of small mobile refractive surface mirrors that route the incident light beams to their destination [47, 48].

Acousto-optic switches are based on the acousto-optic effect of some materials, such as the peratellurite [49] or $LiNbO_3$ [50], where an acoustic wave travelling along the material induces a periodical strain that alters its refractive index. The refractive index modulation induced in the material causes a dynamic phase grating than can diffract light. If the material is isotropic, the diffraction induced by the acousto-optic effect causes beam deflection, and if the material is anisotropic the deflection caused comes along with variation in light polarization.

Other solutions are the thermo-optic switches whose operation consists on the variation of the refraction index of the material by modifying its temperature. This type of switches has a great variety of implementations, but mainly based on using an interferometric mechanism in which the refractive index variation induces a change in the interference condition. This effect facilitates the light switching [51, 52].

Opto-optical switches are based on the intensity-dependent nonlinear effects in optical waveguides, such as the Two-Photon Absorption phenomenon (TPA) [53], the lightwave self action that induces the Self Phase Modulation (SPM) phenomenon and the Kerr Effect that causes the Four Wave Mixing (FWM) and the Cross Phase Modulation (XPM) [54].

Finally, electro-optic switches perform switching by using electro-optics effects. The main technologies are based on Lithium Niobate ($LiNbO_3$) [55], Semiconductor Optical Amplifiers (SOA) [56], Electro-holographic (EH) [57], Bragg Gratings electronically switched [58] and LC. Focusing on the latter, LC switches use different physical mechanisms to steer the light such as polarization management, reflection, wave-guiding and beam-steering (2D or 3D). Main advantages of this technology include no need of moving parts for switch reconfiguration, low driving voltage and low power consumption. In the last years, different devices based on nematic LCs for SI-POF networks have been reported. Some of them are described below.

### 3.1. Optical Switches based on twisted nematic liquid crystals

The polarization rotation is the first configuration used in LC switches [59]. A simple example of a 1x2 switch based on TN-LC is presented in Fig. 6 [60]. Depending on the voltage applied to the TN-LC, the light from the input (Port 1) is guided to one of its outputs (Port 2 or Port 3).

http://dx.doi.org/10.5772/59518

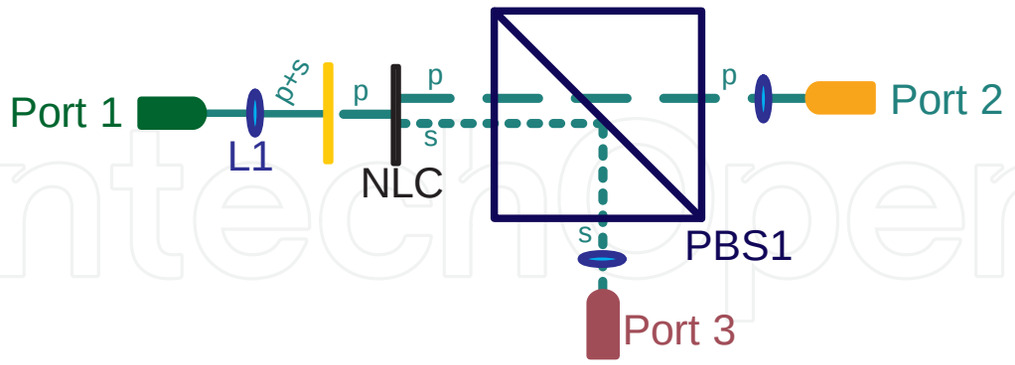


**Figure 6.** Structure of the 1x2 LC optical switch.

As a consequence of the use of the input polarizer for the operation of the TN-LC half of the incoming optical power is filtered. The solution for reducing the insertion losses of the optical switch based on TN-LC cells is by using the polarization diversity method, see Fig. 7. In this technique, the input light is decomposed into its TE (S-Polarized light) and TM (P-Polarized light) components. Both components are treated separately and finally recombined. In this way, the device becomes polarization insensitive, and less insertion losses are expected. The same principle of the reconfigurable multiplexer design reported in the previous section.

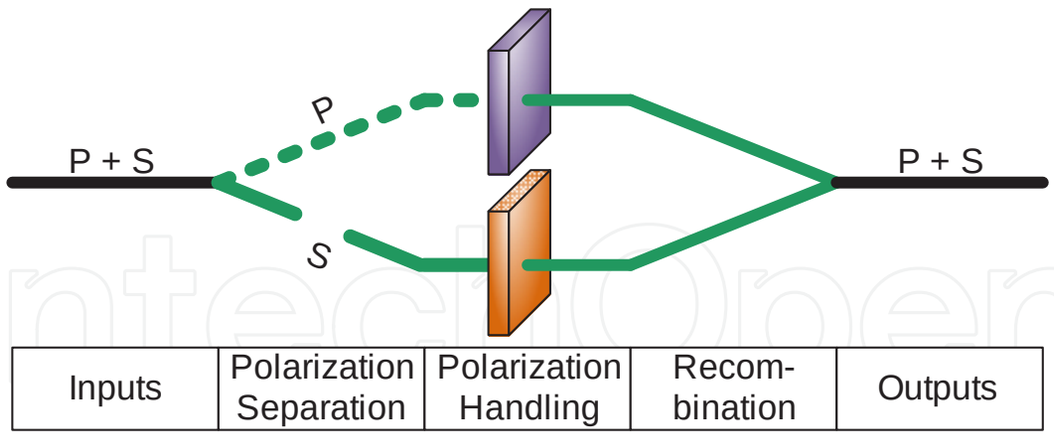


**Figure 7.** Structure of the 1x2 LC optical switch.

Different configurations have been proposed in literature for implementing optical switches based on the polarization diversity method. A polarization insensitive 2 x 2 optical switch based on TN-LC is presented in Fig. 8 [61]. The structure is composed by Polarizing Beam Splitters (PBS1-PBS4), TN-LC cells (NLC1-NLC4), quarter wave plates (Plate 1- Plate 4), and mirrors (Mirrors 1 – Mirror 3). The 2x2 optical switch allows up to three operation modes by applying voltage to the suitable pair of TN-LC cells, see Fig. 9:

– Direct Mode: NLC2 and NLC4 ON; Port 1 → Port 3 & Port 2 → Port 4.
– Crossed Mode: No voltage is applied; Port 1 → Port 4 & Port 2 → Port 3.
– Closed Mode: NLC1 and NLC3 ON; Port 1 → Port 2 & Port 3 → Port 4.

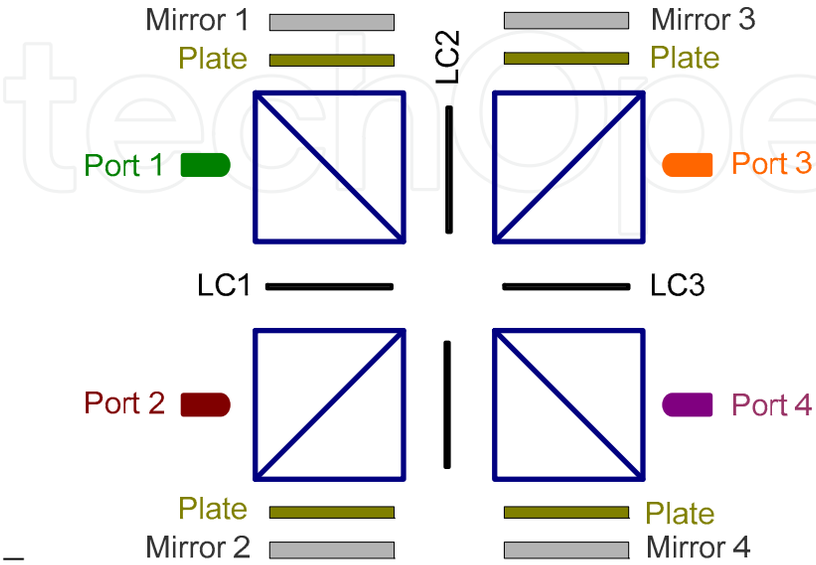


**Figure 8.** Structure of the polarization independent 2x2 LC optical switch.

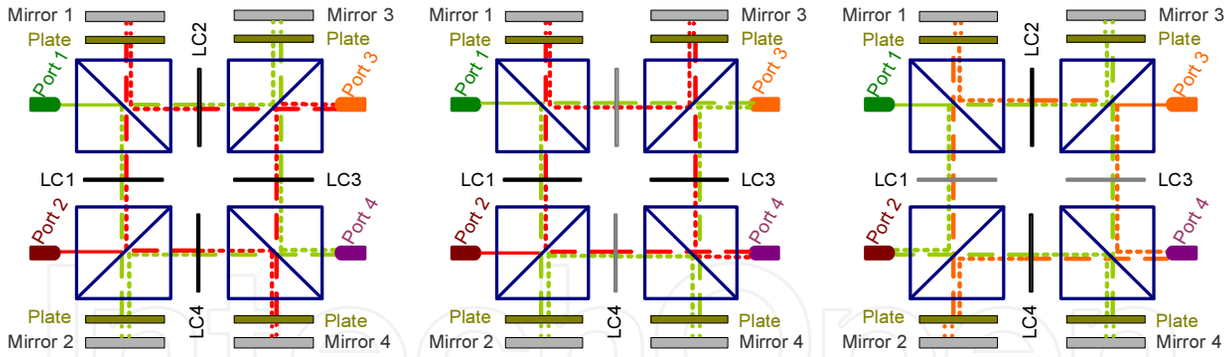


**Figure 9.** Operation modes of the 2x2 optical switch: (a) Crossed, (b) Direct, (c) Closed.

### 3.2. Optical router with output power control

TN-LCs can also be used in routers (LC–OR) based on the polarization diversity method following the same principle of operation as in the case of optical multiplexers. The polarization modulation of a TN cell in combination with space polarization selective calcite crystals or polarization beam splitters (PBS) allows optical space-switching. Fig. 10 shows the structures of a typical 1x2 nematic LC–OR (Fig. 10.a) and a 1x2 nematic LC–OR with independent output power control (Fig. 10.b).

http://dx.doi.org/10.5772/59518

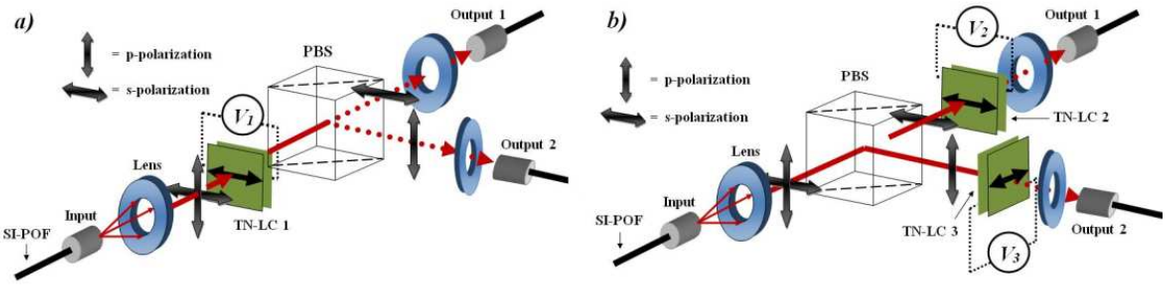


**Figure 10.** a) Structure of a typical 1x2 nematic LC–OR based on polarization diversity and, b) structure of a 1x2 nematic LC–OR with independent output power control.

In the scheme shown in Fig. 10.a, the TN-LC 1 has an input polarizer that changes the polarization state of the transmitted beam depending on the voltage $V_1$. The scheme of Fig. 10.b additionally provides the possibility of stabilizing the optical power that is transmitted by each port. This feature was reported in [62]. In that scheme, TN-LC 2 and 3 have both an input and an output crossed polarizer, with the input polarizer parallel to the respective polarization component transmitted by the PBS. Then, in this scheme each LC cell controls the transmitted power depending on the voltages $V_2$ and $V_3$. Fig. 11 shows an example of the power stabilization capacity of the router reported in [62].

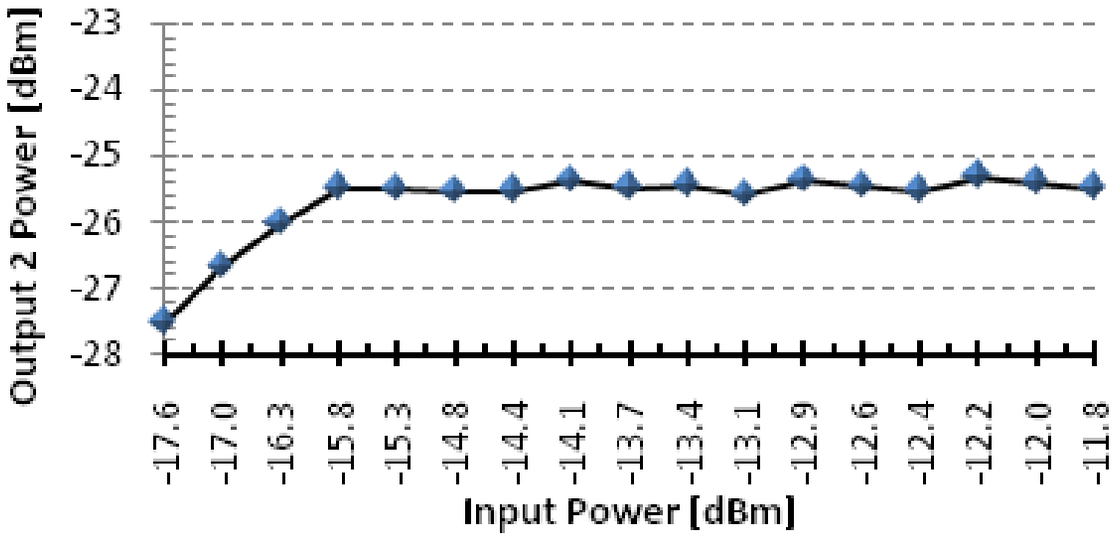


**Figure 11.** Example of the output power control capacity of a 1x2 LC-OR based in polarization diversity. Input power is obtained from a LED source at 650 nm.

LC-OR based on nematic LC cells cannot respond faster than several microseconds. This fact limits its use to telecom and sensor applications for protection and recovery, or optical add/drop multiplexing which need fewer restrictions about switching time, like WDM transport network restoration [63]. However, in the last years, nematic LCs with response times lower

than 3 ms [64] and 2 ms [65], as well as nanosecond response [66] have appeared. And different techniques to reduce the response time below 1 ms [67] have also been reported.

### 3.3. Broadband LC-OR

It is a matter of fact that the performance of a twisted nematic LC-OR is optimum only for specific wavelengths (those given by Mauguin Minima) [68]. Besides, the LC birefringence, which defines Mauguin Minima, is very temperature dependent, requiring temperature compensated designs or controllers. These two limitations can be overcome by replacing the twisted nematic cells (see Fig. 10.a) with optimized polarization rotators (PRs) based on structures of stacked LC cells, as reported in [69]. Figure 12 shows an example of the performance of the broadband 1×2 LC–OR reported in [69].

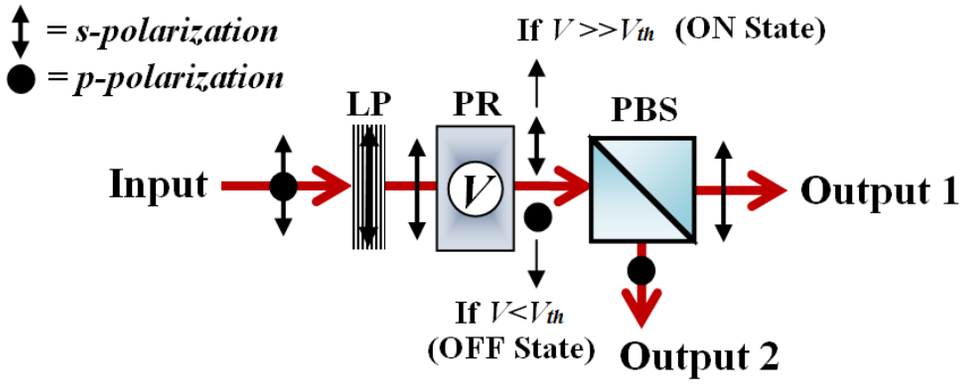


**Figure 12.** Scheme of a broadband 1×2 LC–OR for POF networks.

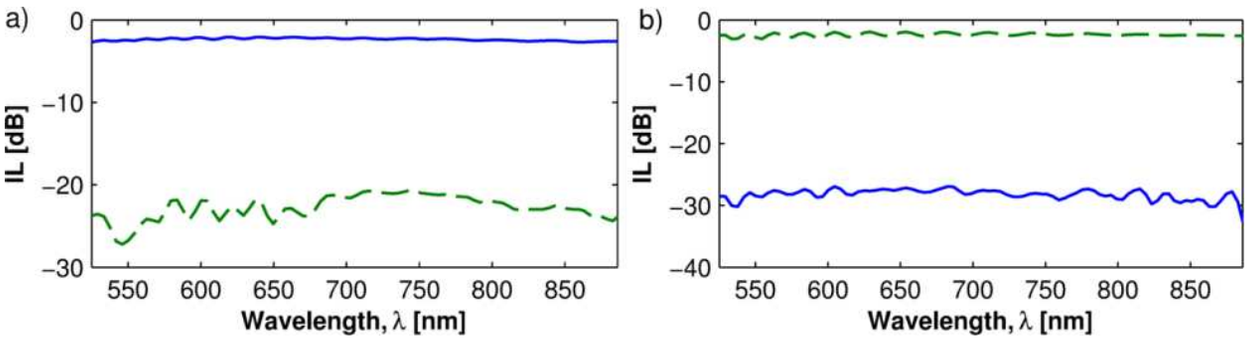


**Figure 13.** Spectral performance of the outputs 1 (dashed lines) and 2 (solid lines) of a broadband 1×2 LC–OR for POF networks in the a) OFF state ($V<<V_{th}$) and b) ON state ($V>>V_{th}$).

The proposed design illustrated above is composed by 3 LC cells and allows a significant improvement of the spectral response of LC optical routers, compared to those previously

http://dx.doi.org/10.5772/59518

reported [43, 62, 70] in a broadband range. The proposed router has quite similar insertion loss values in both outputs in the range from 400 nm to 700 nm, as well as crosstalk values lower than –18.7 dB, as shown in Fig. 13. This performance is required for routing channels in SI–POF–WDM networks uniformly, since in these networks the channels may have wide bandwidths and the proposed grid is very wide, as it was aforementioned. In [69] it has been shown that the router performance is quite constant with temperature changes of up to 10 °C. And it was also demonstrated that it is able to control the split ratio of the output power with good uniformity in the range from 400 nm to 700 nm.

### 3.4. LC wavelength selective switch

A 1×M wavelength selective switch (WSS) is an optical device that allows switching any incoming wavelength from its input port to any of the *M* output ports, without the need for optical to electrical conversions. These devices play a key role in protection and reconfiguration tasks of next generation optical networks. A huge number of approaches to implement WSS have been demonstrated. Some are based on gratings that spatially disperse the input channels, on MEMS, or on LC spatial light modulators [70, 71]. Other approaches use silica-based planar lightwave circuits (PLCs) [72] or ring resonators [73].

Some LC reconfigurable devices for the VIS range have been reported, such as tunable filters [74] or a multifunctional device operating as a switch/combiner/variable optical attenuator [43], as well as a 1x2 WSS [74]. The latter is based on an inverted Lyot filter structure. This configuration allows demultiplexing, switching or blocking any channel through any output port using voltages from 0 to 3 $V_{RMS}$, the same for all the LC cells, with maximum insertion loss of 6 dB, and rejection ratios better than 12 dB. Fig. 14 shows two examples of the eight possible transmission states of the 1x2 LC WSS reported in [74].

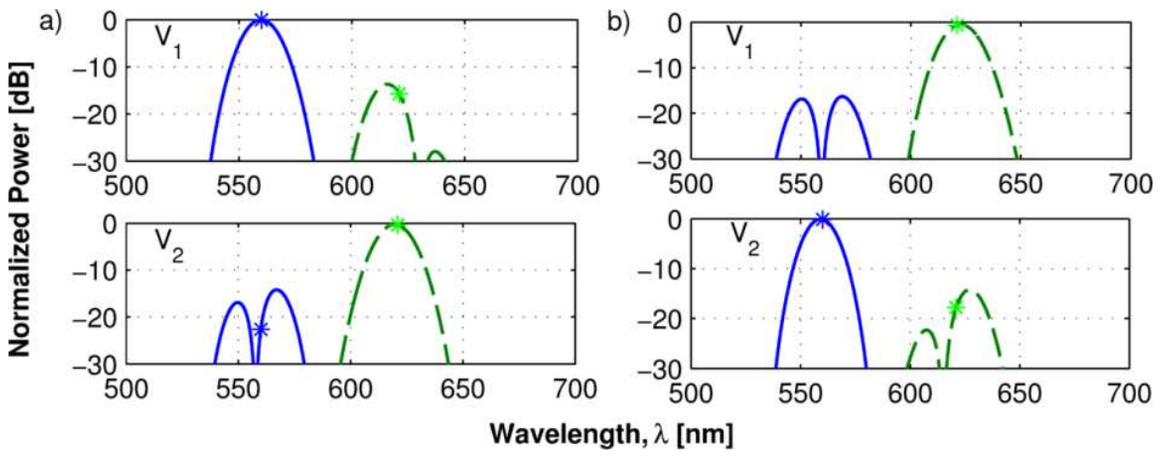


**Figure 14.** Performance example of a 1x2 LC WSS considering 2 LED channels at 589nm (solid lines) and 650nm (dashed lines) with 20 nm full width at half maximum. Where: a) output 1 and b) output 2. V1 = 1.18 $V_{RMS}$ and V2 = 0.21 $V_{RMS}$.

## 4. Optical filters in POF technology

Optical filters are basic components as part of routing devices for optical communications networks. Optical interleavers are filters that due to their periodicity: a) separate an incoming spectrum into two complementary set of periodic spectra (odd and even channels), or b) combine them into a composite spectrum. Filters and interleavers play a key role in dense wavelength division multiplexing (DWDM) systems, usually employed in gain equalization, dispersion compensation, prefiltering, and channels add/drop applications.

Literature provides many optical filtering and interleaving devices. Some filters are based on birefringent structures such as the Lyot and Solc filters due to their low dispersion, high reliability, easy fabrication process and low cost [75], with recent applications in VIS for POF networks [69, 74]. However, these solutions mainly operate in DWDM systems (infrared range). In this section, the basic structures of birefringent filters (Lyot and Solc) are presented and compared against birefringent filters designed in the Z transform domain, which can be used in future WDM-POF systems.

### 4.1. Birefringent filters

Birefringent filters base their operation on the interference of an input light beam with multiple delayed versions of itself. Typically there are two types of birefringent filters, the Lyot and Solc. An excellent discussion of both types of filters can be found in [76]. In general, a Lyot filter consists of a set of delay stages composed by retarder plates of different widths between polarizers, as the 3-stage Lyot filter shown in Fig. 15.a. The optical axis of the retarder plates are at 45º with respect to the polarizers (azimuth angle) and each stage has twice the delay (Γ) of the previous one. Focusing on the second approach, Solc filters eliminate the need of Lyot filters for using multiple polarizers. Solc filters consist of a stack of M retarder plates between only two linear polarizers. In this case, all the retarder plates have the same delay and each one are at a specific azimuth angles, $\alpha_{1,..}$ $\alpha_M$, e.g. a fan Solc filter has parallel polarizers ($\alpha_A$ = 0º) and $\alpha_1 = \alpha$, $\alpha_2 = 3\alpha$, $\alpha_3 = 5\alpha$,..., $\alpha_M = (2M\text{-}1)\alpha$, being $\alpha = 45º/M$, see Fig. 15.b.

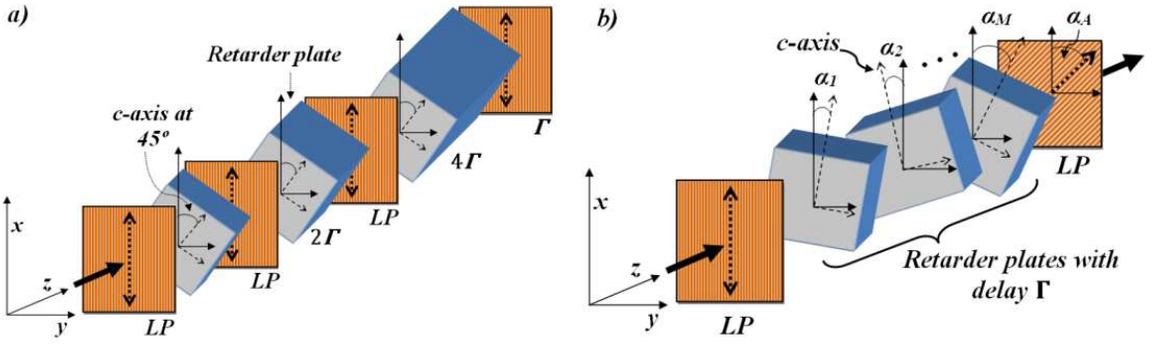


**Figure 15.** General structures of: a) Lyot filter of 3 stages and b) Solc Filters

http://dx.doi.org/10.5772/59518

Now, let us compare Lyot and Solc filters. For example, 3-stage Lyot filters require 4 polarizers and the equivalent of 7 retarder plates with delays Γ, as shown in Fig. 15.a. In contrast, a Solc filter with the same number of retarder plates requires only 2 polarizers. From this point of view Solc filters are a more interesting choice than Lyot filters. However, as is shown in Fig. 16, the adjacent side lobes suppression is better for the case of Lyot filters.

However, the potential of the structure of Solc filters can be exploited by placing the retarder plates illustrated in Fig. 15.b at arbitrary azimuth angles, in a type of filters called lattice or birefringent filters. Birefringent filters can be designed by using optimization methods or in the Z-transform domain, by using their relation with FIR (Finite Impulse Response) filters. A detailed method for transform FIR filters into birefringent filters can be found in [75]. For example, an arbitrary birefringent filter of seven retarder plates, obtained from a $7^{th}$ order FIR filter, is presented in Fig. 16. The azimuth angles of the retarder plates are: $\alpha_1 = 6.07^{\circ}$, $\alpha_2 = 15.18^{\circ}$, $\alpha_3 = 28.65^{\circ}$, $\alpha_4 = 45.00^{\circ}$, $\alpha_5 = 61.35^{\circ}$, $\alpha_6 = 74.81^{\circ}$, $\alpha_7 = 83.92^{\circ}$ and $\alpha_A = 0^{\circ}$. This filter performs a uniform suppression of the adjacent side lobes with a maximum value better than both the Lyot and Solc filters. It could even be designed to have a narrow bandpass. Birefringent structures are a versatile solution for designing devices for POF WDM networks due to their reconfiguration capacity, since they can be easily manufactured with LC technology, and flexibility, since any FIR filters synthesis method can be used [75].

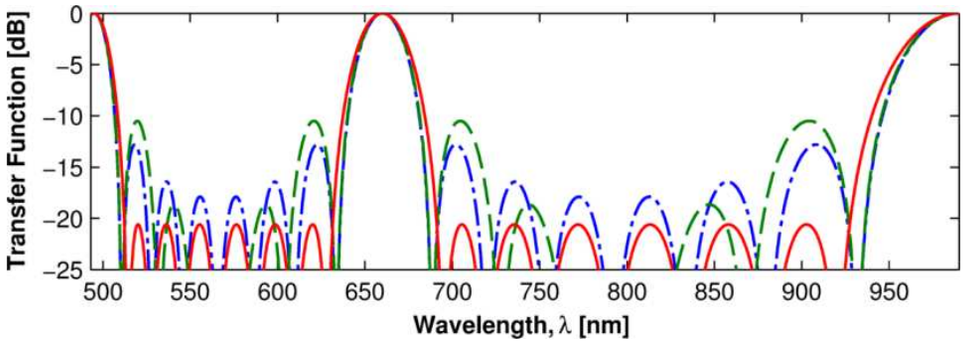


**Figure 16.** Transfer functions of different birefringent filters: 3 stages Lyot Filter (dash-dot line), Solc filter with 7 retarder plates (dashed line) and arbitrary birefringent filter of 7 retarder plates designed in the Z-transform domain (solid line). Retarder plates with $\Gamma = 2\pi \times 1.98\mu m/\lambda$ are considered in all the filters.

It should be mentioned that demultiplexer devices may be easily built up by combining the switches and filter schemes described in former sections or by using filter plus the addition of POF splitting devices.

## 5. WDM approach using Polymer Optical Fiber Bragg Gratings (POFBGs)

As previously stated, one solution to increase the POF's bandwidth, and thus its capacity, is the transmission of information over more than just a single wavelength. This is what is known the WDM approach. This architecture not only has been proved to be suitable for transmission information purposes but also has been demonstrated to be fully compatible with the inter-

rogation of multiple remotely located intensity-based optical fiber sensors, thus taking advantage of the power loss reduction as well as the high scalability provided by the use of WDM devices.

The basis of WDM systems is the spectral characteristics of the optical multiplexers and demultiplexers which are used in the fiber plant instead of optical power splitters. Moreover, within these approaches, FBGs are usually employed both for monitoring purposes or providing an effective and compact strategy to operate in reflective configuration [77, 78]. These devices are a wavelength-selective filter fabricated inside the core of an optical fiber for which the reflected wavelength changes under the influence of external perturbations [79]. First FBGs were traditionally manufactured on silica optical fiber. More recently, FBGs have been inscribed into SI-POF [80] and microstructured Polymer Optical Fiber (mPOF) [81] based on PMMA, leading to what is called polymer optical fiber Bragg gratings (POFBGs). The reason for this development is the exploitation of polymer benefits such as larger elastic limit, higher maximum strain limit, larger temperature and humidity responses and low cost compared to silica, while maintaining the benefits of FBGs. And this fact is also true when considering FBGs as optical sensing elements [82, 83]. In addition, polymer reveals to be intrinsically more biocompatible than silica for as it may be used for *in vivo* biomedical applications where the use of glass is inappropriate due to danger from breakages. Nevertheless, limited effort has been directed towards synergizing biocompatible POF-based photonic sensing with the WDM interrogation method that allows multiplexing by the use of FBGs, with just a few exceptions [84]. The main underlying reason behind this lack of development is the mismatch between the optimum operating wavelength regions of POFs and the optical devices exploited for telecommunications purposes as aforementioned at the beginning of this chapter.

In this section, we intend to bridge the gap between a WDM compatible topology and the use of novel POFBGs by analyzing the feasibility of a hybrid silica-POF WDM network for remotely addressing multiple intensity-based self-referenced fiber-optic sensors. The proposed topology is compatible with the target of developing a single optical broadband network architecture which is capable of carrying many types of services without mutual interference nor design compromises. It may include the access network domain (e.g. FTTx) as well as up to the indoor scenario with the aim of a full converged network solution. This solution will open up the path for the development of converged WDM POF communication networks in the near future. Moreover, potential medical environments and biomedical applications based on all-optical POF-based solutions are also targeted taking advantage of the intrinsic POF biocompatible characteristics.

The proposed self-referenced hybrid topology above described is illustrated in Fig. 17. The novelties of this configuration in comparison with previous works [78, 85] are: a) the combination of silica- and polymer- FBGs (the latter may be used for *in vivo* scenarios or just simply at the patient's vicinity if the target is a biocompatible optical system for medical applications); b) the usage of a single reference FBG; and c) an improved centralized monitoring unit (that can be remotely located up to units of km) which includes virtual instrumentation techniques and data processing. A broadband light source (BLS) is, either internally or externally, modulated at a single frequency ($f$). This modulated signal is launched into the remote sensing

http://dx.doi.org/10.5772/59518

points via a broadband circulator and a Coarse Wavelength-Division Multiplexer (CWDM). Each remote sensing point located consists of a sensing POFBG placed after the fiber-optic sensor (FOS). A single silica FBG is located before the CWDM acting as a reference channel for the topology. Let assume the central wavelengths of the reference and sensing FBGs to be $\lambda_{Si}$ and $\lambda_{POF}$, respectively. The broadband optical circulator receives the reflected multiplexing signals from the reference and the sensor channels, in which the sensor information is encoded. At the remote monitoring unit, the optical signal is demultiplexed by a CWDM device and distributed to an array of photodetectors (PD) by means of a data acquisition board (DAQ) together with a band-pass filter (BPF), used to eliminate noise from all signals at frequencies outside the system frequency. Then, a phase-shift is applied to the reference and sensor digital signals. Finally, a virtual lock-in amplifier is used to interrogate all available sensor channels. A measurement parameter can be defined, $\varphi_K$, corresponding to the output phase of the signal for different phase-shifts (virtual delays) at the reception stage, see Eq. 1.

$$\varphi_K = \tan^{-1}\left[\frac{-\left(\sin\theta_{Si} + \beta_k \bullet \sin\theta_{POF_k}\right)}{\cos\theta_{Si} + \beta_k \bullet \cos\theta_{POF_k}}\right] \tag{1}$$

where $\theta_{Si}$ and $\theta_{POF_k}$ are, respectively, the phase shifts for the reference and each sensor signal $k$, and $\beta_k$ is relates to the optical power received at the remote central unit being a function of the modulation index, the reflectivity of the silica FBG and the photodetector responsivity (for both sensing and reference wavelengths), the sensor power loss modulation, the insertion loss of the CWDM device, and the insertion loss related to the reflectivity, intrinsic attenuation and connectorization of the POFBGs. Further details of the mathematical framework can be seen in the works reported in [78, 86]. Parameter $\varphi_K$ is insensitive to power fluctuations except for the sensor modulation thus performing as a self-reference measurement parameter. Its performance, i.e. linear behavior, maximum sensitivity, etc., is directly related to the digital phase-shifts applied at reception.

To test the feasibility of the topology shown in Fig. 17, a 2-sensor network was analyzed by modulating the BLS at f=1kHz by an acousto-optic modulator. The optical power was launched into the configuration via a broadband circulator. One silica FBG was used for reference purpose, being placed before the CWDM mux/demux. Its central wavelength and reflectivity were $\lambda_{Si}$=1550nm and 49%, respectively. A POFBG in 150μm cladding diameter few-moded mPOF was used for each remote sensing point, with central wavelengths $\lambda_{POF_1}$=1525.2nm for $FOS_1$ and $\lambda_{POF_2}$=1567.0nm for $FOS_2$. Their reflectivities were 27 % and 36 %, respectively. A singlemode VOA was used to emulate the sensor response and for calibration purposes. The reflected signals were demultiplexed by a CWDM and detected by three amplified InGaAs detectors. The amplifier gain was fixed at 70 dB for all measurements. A 14-bit low-cost DAQ was used to convert the electrical signals from the photodetectors to digital signals. Virtual instrumentation techniques were developed to implement the bandpass filter, the phase-shifts and the lock-in amplifiers at the reception stage.

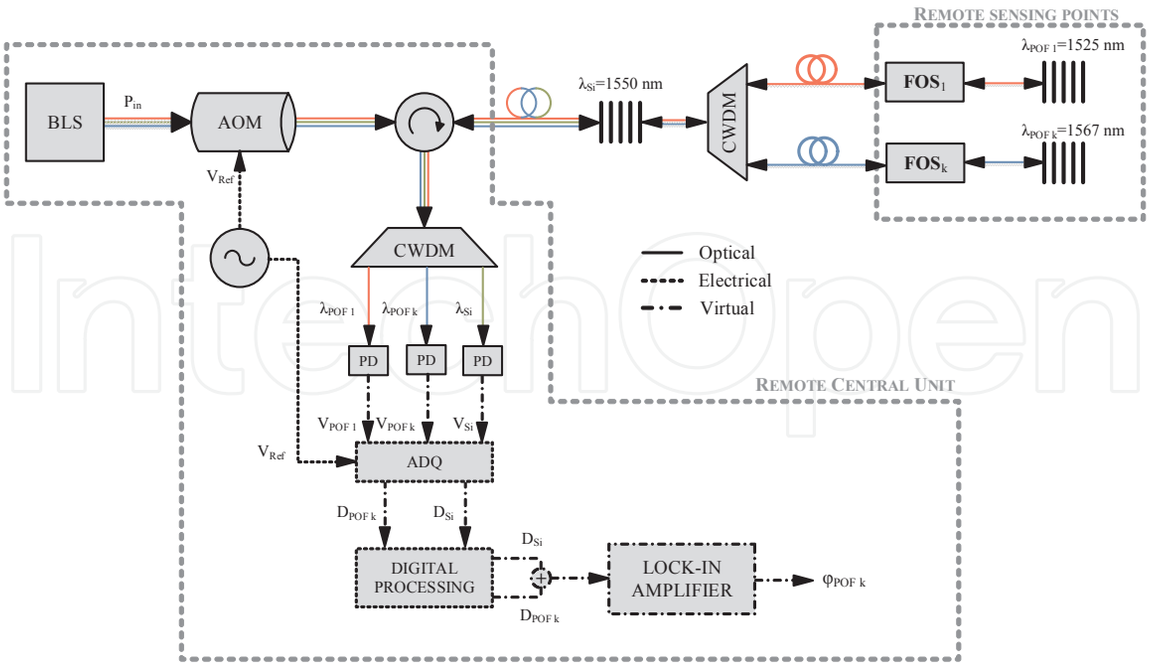


**Figure 17.** Hybrid silica-POF WDM self-referenced topology for remotely addresing generic remote sensing points located at the patient's vicinity. Fiber-optic sensor (FOS).

The self-reference property was tested inducing power fluctuations in the modulated optical source through a VOA. Fig. 18 showed no changes in $\varphi_K$ values after inducing 10 dB of power attenuation. It is worth mentioning that the proposed topology performs no noticeable crosstalk between adjacent channels. This means that both (or more) sensors could be interrogated simultaneously without mutual interference because of the high channel isolation of the CWDM demultiplexer. Experiments were carried out for the following phase shifts at the reception stage: $\theta_{Si}=0.83\pi$, $\theta_{POF\,1}=0.33\pi$.

The performance of the proposed topology was further investigated obtaining resolution values far below than that of provided by most of the POF intensity based sensing solution reported in literature, and particularly for biomedical applications. Another interesting point is computing the power budget, which provides information about the maximum remote interrogation reaching distance and/or the maximum insertion losses only for sensing purposes. At the most restrictive sensing wavelength (in terms of reaching distance), a maximum length of 11 km could be obtained. For this calculation, a FOS power variation of 6 dB was considered, high enough to cover any biomedical input magnitude span. However, this reach distance can be easily improved by launching more optical power into the system, using optical devices with better insertion loss performance or using a more efficient technique to connect POFBGs. The aforementioned reaching distance could provide a remote monitoring service unit fully compliant for both short-reach networks (typically less than 1 km), i.e. LANs and in-building/in-hospital networks as well as suitable for medium reach-distances (typically up to 10 km). Furthermore, the latter value ensures applications in inter-hospital networks or to provide a convergent all-optical and straightforward connection between patient's homes and

a general practice service for telemedicine purposes. It should be mentioned that the above reaching distances are unbeatable if an all-POF-based optical network is intended to be deployed and a hybrid approach should be considered. Following this analysis, it can be concluded that the proposed topology do not provide limitations thus serving as the bottleneck of a multiple remote sensing scheme.

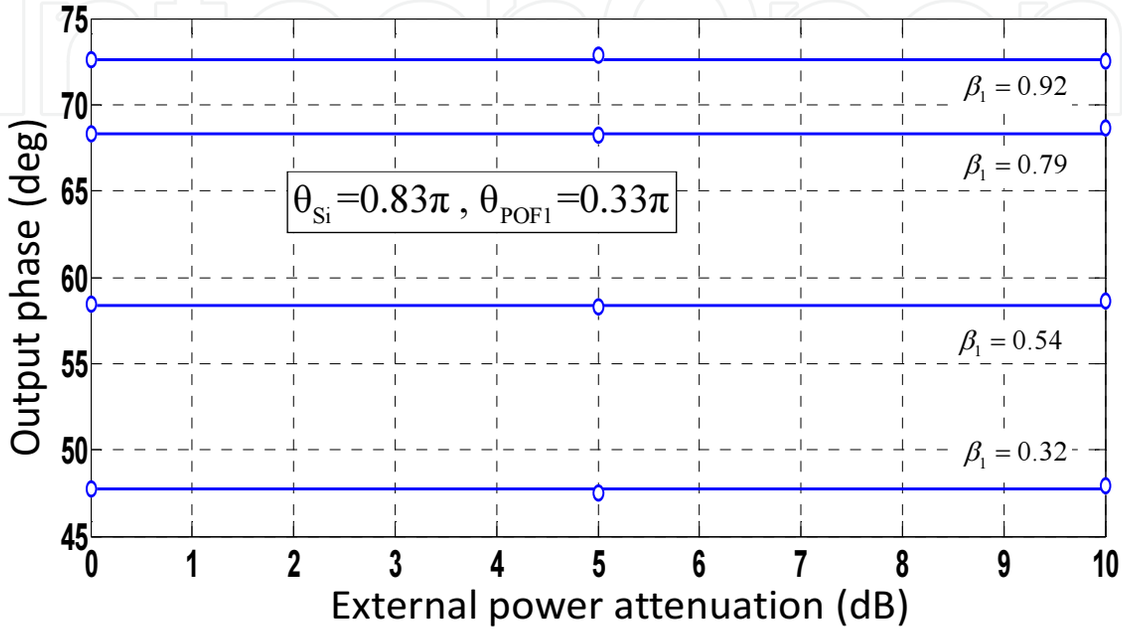


**Figure 18.** Output phase $\varphi_1$ self-reference test versus power fluctuations for different values of sensor losses at the remote sensing point addressed by $\lambda_{POF\,1}$.

## 6. WDM extension over PF GIPOF links

In this section a comparison between the achievable capacity over a single fiber channel and over a WDM PF-GIPOF-based approach will be presented. It has been previously stated that a typical WDM optical communication link requires both a multiplexer and a demultiplexer. However, the addition of POF-WDM multiplexer and demultiplexer devices, results in a bit-rate penalty as the available optical power on the system decreases due to their insertion losses. To establish the channel capacity comparative, a bit loading algorithm for DMT modulation format over PF-GIPOF has been considered. New power margin resulting from the additional losses considered in the system due to the WDM over POF approach are analyzed demonstrating the feasibility of PF-GIPOF WDM systems.

The resulting theoretical Shannon capacity of an optical fiber channel can be calculated if its $f_{3dB}$ is known [14], modeled as a Gaussian low-pass filter. Therefore, from measurements of frequency response of different PF-GIPOF lengths, 3dB bandwidths can be obtained, and so their theoretical capacity limits operating in a single channel. This type of

fiber has been demonstrated to enable robust 2GbE (GbE, Gigabit Ethernet) and 10GbE baseband transmission over short reach distances ranging from 25m up to 100m for different link scenarios [87], even at OverFilled Launching (OFL) condition. These values are considered as an underneath estimation of the transmission limit of PF-GIPOFs as complex modulation formats, restricted mode launching schemes, equalization techniques or simultaneous data transmission over high-order latent PF-GIPOF passbands can be applied to enhance its aggregated capacity [88-90].

Previous works have studied, analyzed and modeled the PF-GIPOF frequency response taking into account most of the parameters that affect the latter. Some noteworthy PF-GIPOF frequency response measurements are shown in Fig. 19, in which a good agreement between experimental results and the theoretical curves predicted by the model is observed. This figure shows the measured and theoretical frequency responses for a 50m, 75m and 100m-long 62.5μm core diameter PF-GIPOF link with OFL condition and employing a Fabry-Perot laser source operating at 1300nm. Further details of the mathematical framework and experiments are reported on [91] for the benefit of the readers.

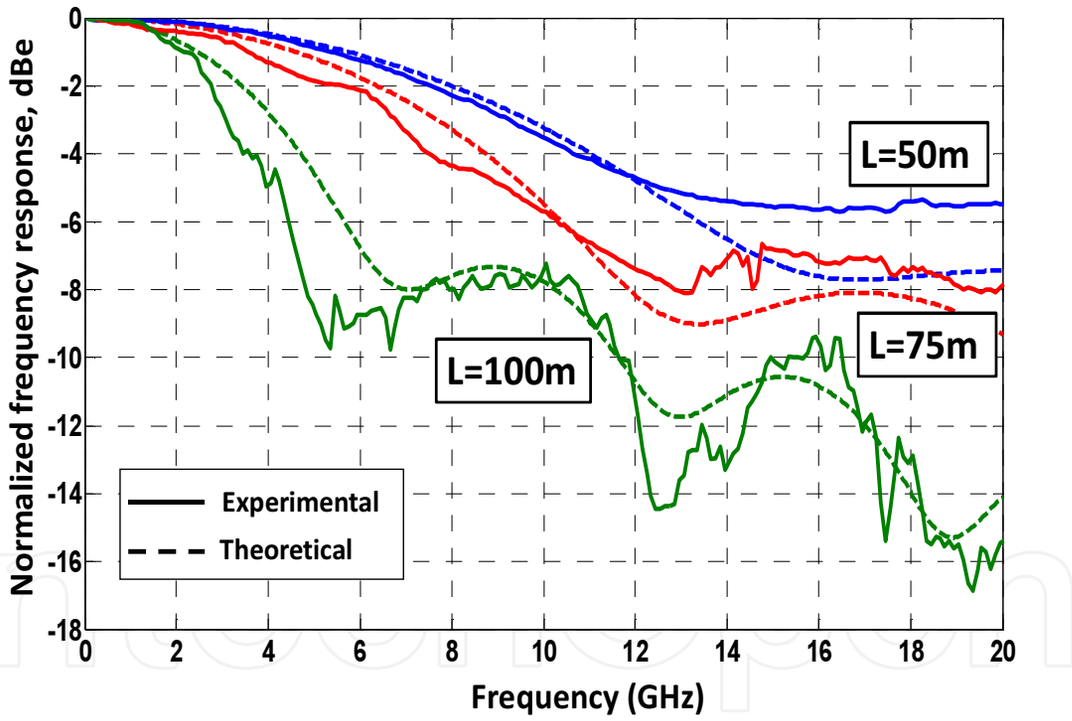


**Figure 19.** Measured (solid line) and theoretical (dashed line) electrical responses for different 62.5 μm core diameter PF-GIPOF lengths.

From frequency response measurements, as shown in the above figure, the 3dB baseband bandwidth can be easily identified and, therefore, the channel capacity can be calculated. The PF-GIPOFs used are commercially available from Chromis Fiber with an attenuation of 55dB/km at 1300nm. For the frequency response measurements, a FP laser diode used as transmitter was externally AM modulated with a RF sinusoidal signal (up to 20GHz of

http://dx.doi.org/10.5772/59518

modulation bandwidth) by means of an E/O Mach-Zehnder modulator (16GHz bandwidth). An InGaAs-photodetector (22GHz bandwidth) is used as receiver. Bandwidth limitation from both transmitter and receiver can be neglected for links >50m. The channel capacity for each length, is calculated based on the transmission characteristics listed below, and is displayed in Table 1. For some applications, e.g. home network Ethernet transceivers, eye safety operation is required and a limited averaged transmitted optical power of 0dBm has been considered.

| Length (m) | Measured electrical -3dB bandwidth (GHz) | Capacity (Gbps) | a) Average transmitted optical power=0dBm |
|---|---|---|---|
| **25m** | 18.4 | 590.5 | |
| **50m** | 9.2 | 299.6 | b) Fiber attenuation @1300nm= 55dB/km |
| **75m** | 6.7 | 208.8 | |
| **100m** | 3.2 | 101.9 | c) Clipping factor=3 |
| **125m** | 1.7 | 54.4 | |
| **150m** | 1.2 | 36.9 | d) Noise equivalent power: NEP=17.3·$10^{-12}$ W/√Hz |

**Table 1.** Calculated theoretical capacity over 62.5μm core diameter PF-GIPOF, at 1300nm.

However, this capacity analysis from the frequency response may result in large discrepancies at frequencies beyond the 3dB point and the PF-GIPOF has some latent high-order passbands [88]. Consequently, the Gaussian low-pass approximation reveals itself as a pessimistic approximation of the PF-GIPOF channel capacity, and expected capacity values of PF-GIPOF can be larger than those calculated in Table 1, even more if Restricted Mode Launching (RML) schemes are applied to the injection of light into the fiber.

On the other hand, DMT allows the possibility to allocate the number of bits and energy per subcarrier according to its corresponding signal-to-noise ratio (SNR), typically known as bit-loading. To compute rate-adaptive bit-loading for the DMT over PF-GIPOF consideration Chow's algorithm has been implemented [92]. Initially, all subchannels were loaded with 4 information bits each. Table 2 shows the theoretical results on capacity when applying DMT over a single channel, based on the measured frequency response values up to 150m-long PF-GIPOFs. Compared to the results given in Table 1, it can be seen that for the shortest length (25m), the numerically computed capacity value is lower than theoretical counterpart. This result from bandwidth limitation of the external modulator bandwidth, considered in the computation. From lengths > 50m, the computed capacity is larger because the PF-GIPOF frequency response dominates over other bandwidth limitation factors. Due to the bandwidth limitation of the PF-GIPOF link itself, the signal-to-noise-ratio decreases for higher frequencies. Bit allocation resulting from the bit loading is shown in Fig. 20 for a 100m- and 150m-long PF-GIPOF single channel link, respectively.

| Length (m) | Numerical DMT over PF-GIPOF Capacity (Gbps) |
|---|---|
| **25m** | 577.1 |
| **50m** | 380.0 |
| **75m** | 276.9 |
| **100m** | 164.1 |
| **150m** | 77.1 |

Note: targeted BER=$10^{-3}$

**Table 2.** Theoretical DMT capacity over 62.5μm core diameter PF-GIPOF, at 1300nm.

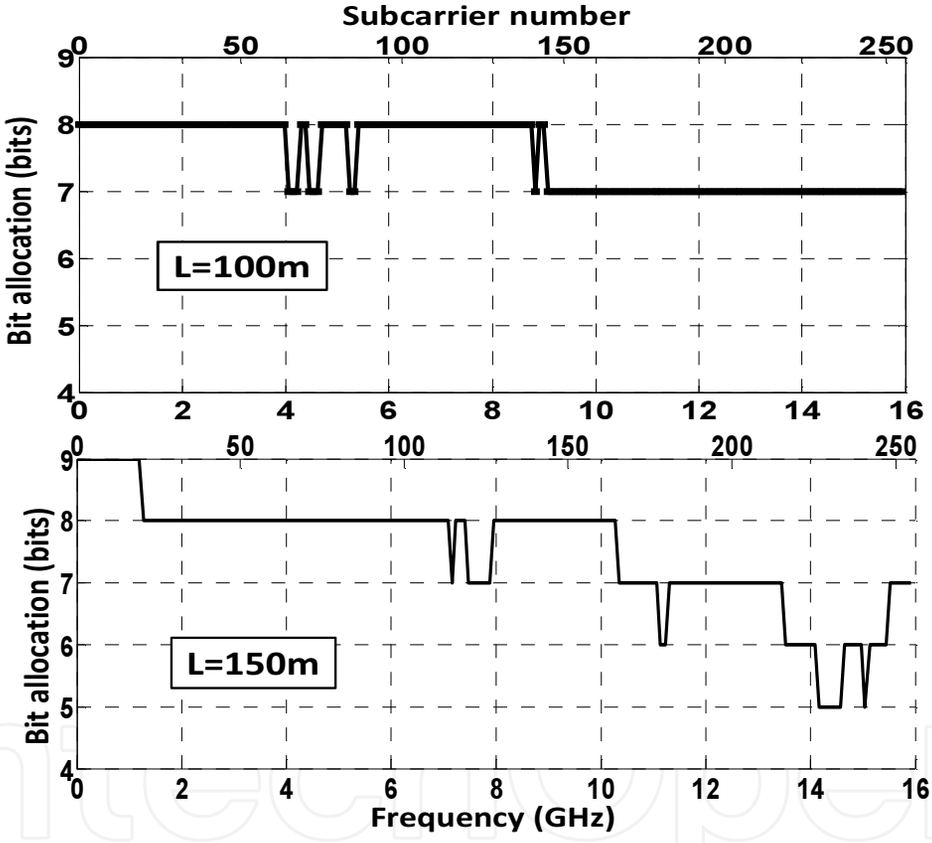


**Figure 20.** Bit allocation per subchannel, resulting from bit-loading at 100m and 150m.

It has been previously stated that for flexible high capacity GIPOF optical networks, applying the WDM approach seems to be necessary. Apart from the physical transmission characteristics of the PF-GIPOF, it is equally important to consider the optical components introduced to deploy advanced WDM-based optical architectures. The addition of these POF WDM multiplexers and demultiplexers limits the available optical power budget within the fiber link thus resulting in a bit-rate penalty. This is due to the fact that the OSNR (Optical Signal-to-Noise ratio) of the system is being reduced, and so the fiber transmission capacity.

http://dx.doi.org/10.5772/59518

To establish a comparison between the PF-GIPOF single channel operation and its WDM extension a 4-$\lambda$ WDM approach has been considered. Regarding the latter, the PF-GIPOF transmission capacity must be recalculated from: a) the new bit loading resulting from the DMT modulation scheme and, b) the restriction on power margin resulting from the new losses considered in the system due to the addition of the mux/demux devices in the optical link. An insertion loss for a future PF-GIPOF 4-$\lambda$ multiplexer/demultiplexer device of around 2dB per channel [93, 94] is considered. Such a performance is better in terms of insertion loss with respect to PMMA-GIPOF based splitters which can provide insertion losses greater than 6dB (in the symmetric-case) [95]. Consequently, the power budget of the WDM system, consisting of one PF-GIPOF based multiplexer or demultiplexer device at each side of the optical fiber link, results in a 5dB power reduction per channel, if an optical crosstalk of 1dB is also considered. It is worth mentioning that some authors have evaluated power penalties close to 2.4dB when combining a 62.5μm core diameter PF-GIPOF and WDM devices based on 50μm core diameter MMF [90]. Set of Fig. 21 shows the theoretical bit loading including the afore-mentioned restriction in power budget due to the 4- $\lambda$ WDM approach.

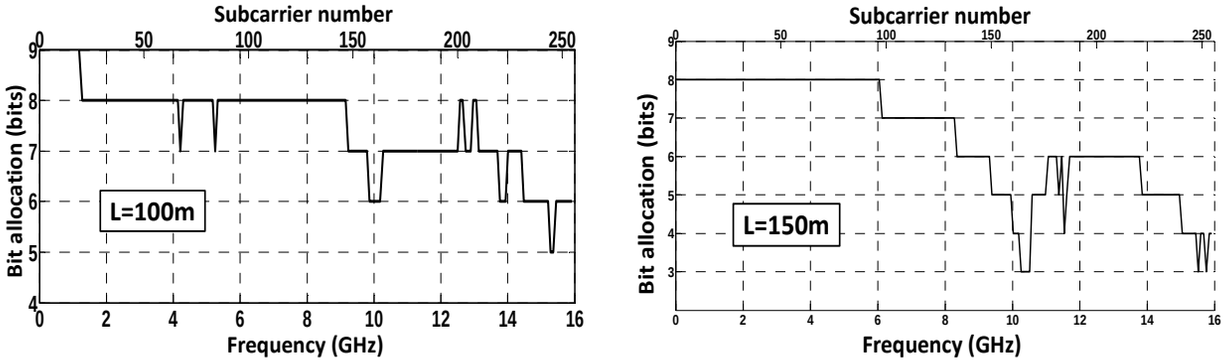


(a) (b)

**Figure 21.** Theoretical bit loading for the 4- $\lambda$ WDM approach over PF-GIPOF. (a) 100m ; (b) 150m.

The corresponding aggregated WDM capacity is summarized in Fig. 22 and compared to the single channel operation. The achievable capacity of a single-$\lambda$ WDM system does not reach the best single channel results. For a single channel operation more than twice the capacity compared to the single-$\lambda$ capacity in the WDM approach. Therefore, assuming a 4-$\lambda$ WDM system using the full available optical power and with similar bit rate transmission performances in each channel the total achievable capacity would overcome the OSNR and bit-rate limitation due to the optical losses introduced in the power budget of the system. It is also noticed that for longer PF-GIPOF lengths the ratio between transmission capacities for single channel and single- $\lambda$ operation diminishes. This fact is attributed to differential mode attenuation (DMA) together with mode coupling effects in PF-GIPOF that leads to a sub-linear increase dependency of the fiber bandwidth regarding its length. This favours the resulting transmission capacity.

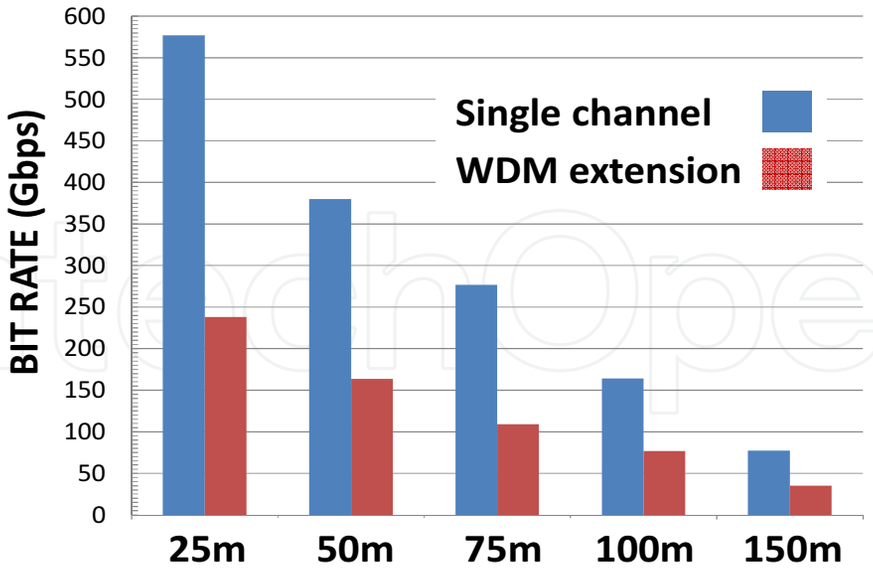


**Figure 22.** Comparison of single channel operation and WDM extension over 62.5μm core diameter PF-GIPOFs.

On the other hand, capacity values for a 50μm core diameter PF-GIPOF following the same procedure and under the same constraints are also shown (from its frequency response measurements). Greater capacities can be achieved as increasing the core diameter due to the presence of strong mode coupling effects and less modal noise effect, as shown in Fig. 23.

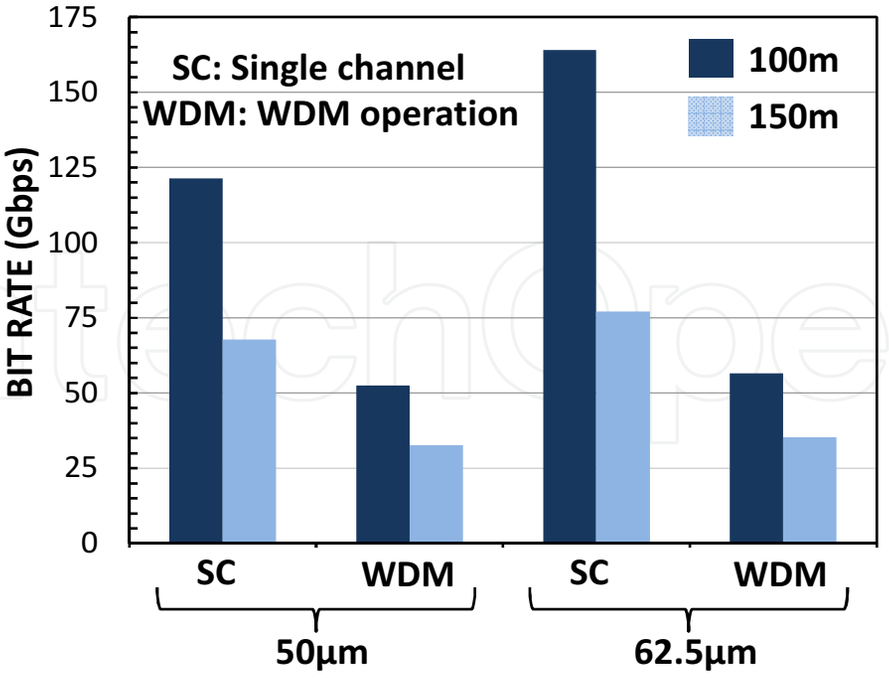


**Figure 23.** Comparison of single channel operation and WDM extension over a 100m- and 150m-long link, at 1300nm, for different core diameter PF-GIPOFs.

http://dx.doi.org/10.5772/59518

## 7. Discussion and conclusions

Applying WDM can further enhance the transmission capacity via POF systems. This chapter is intended to bridge the gap of WDM POF-based networks for in-home deployments, where POFs have become a competitive and low-cost solution as a physical medium infrastructure. In-home link lengths are relatively short thus leading to a more relaxed requirements regarding bandwidth x length product and attenuation per unit length, respectively. However, due to the continuous increase of bit-rate demands from end-users for multimedia services new techniques oriented to overcome the POF bandwidth limitation are being required. Beyond complex modulation formats in which the main goal is to provide a single channel communication link with a high spectral efficient (i.e. bit/Hz), one potential solution to expand the usable bandwidth of POF systems is to perform multiple channels over a single POF. This is known as the WDM approach.

Nowadays, WDM is well-established in the infrared transmission windows for silica optical fibers, but this technique needs to be adapted to VIS for POFs due to their spectral attenuation behavior. And novel WDM POF devices and network topologies are necessary to a final success of POF in-home penetration. These devices include POF multiplexers/demultiplexers, variable optical attenuators, interleavers, switches, POFBGs and/or optical filters to separate and to route the different transmitted wavelengths. And an easy-reconfigurable performance can be an additional feature among all the spectrum of future designed and manufactured devices for the WDM POF solution, with the aim of increasing the flexibility of multiplexing, demultiplexing, switching and routing optical signals as well as modifying the optical network if required. Moreover, devices that can perform different functionalities are interesting in terms of reducing the power consumption and insertion losses. It is also important to follow the progression in stable and low cost light sources in the visible range, apart from 650nm, to successfully achieve the WDM POF implementation. And new devices, benefiting from nanoparticles principles to reach novel plasmonic switches among others.

Anyway, progresses in these POF devices for the WDM approach have been discussed. They can operate in the visible range as POFs do. Among the different technologies, within this chapter two multiplexers based on TN-LC have been introduced. The use of this technology has been demonstrated to provide several advantages as they do not have mobile parts, need low excitation voltages and have a low power comsuption. In addition, a reconfigurable optical multiplexer based on PDLC has been presented which can also acts as a variable optical attenuator. It has also been designed switches operating in a broadband range with a uniform spectral response and low thermal dependence. Birefringent structures are proved to be a versatile solution for designing devices for POF WDM networks due to their reconfiguration capacity, since they can be easily manufactured with LC technology, and flexibility, since any FIR filters synthesis method can be used.

On the other hand, the capabilities of novel POFBG devices to be compatible with WDM topologies for both sensing and communication schemes have been addressed. High scalability

and power budget enhancement in comparison with all POF based network solutions is achieved due to the use of off-the shelf silica WDM devices in combination with POFBGs. Reaching distances of tens of km can be easily achieved with the proposed topology fully compliant with both short-reach networks (typically less than 1 km), i.e. LANs, in-building/in-home networks etc. as well as medium-reach distances (typically up to 10km) covering the access domain. The above reaching distances are unbeatable if an all-POF-based WDM optical network is intended to be deployed and a hybrid approach should be considered.

Finally, to mitigate both the impact of the high attenuation as well as the limited bandwidth of standard POFs recently developed PF-GIPOFs should be also considered. This fiber type outperforms these two features compared to their Step-Index and PMMA-based counterparts, respectively. Nevertheless its achievable capacity under the WDM-GIPOF approach must be analyzed. A future 4-$\lambda$ WDM-GIPOF deployment is studied showing that its total achievable capacity can overcome the OSNR and the bit-rate limitation due to the optical losses introduced in the power budget of the system due to the addition of future GIPOF-based WDM devices.

We believe the results reported in this chapter may encourage the development of WDM-POF networks and low insertion loss POF-based WDM devices opening up the path for future in-home systems at very high bit rates. However, further improvements on mux/demux manufacturing would make WDM-POF systems a future-proof and feasible solution for in-home/building networks to attend end-users' high-speed demands.

## Acknowledgements

The work comprised in this document has been developed in the framework of the activities carried out at the Displays and Photonics Applications group (GDAF) at Universidad Carlos III de Madrid.

This work has been supported by the Spanish Ministry of Economía y Competitividad under the grant TEC2012-37983-C03-02.

## Author details

David Sánchez Montero*, Isabel Pérez Garcilópez, Carmen Vázquez García,
Pedro Contreras Lallana, Alberto Tapetado Moraleda and Plinio Jesús Pinzón Castillo

*Address all correspondence to: dsmontero@ing.uc3m.es

Electronics Technology Department, Universidad Carlos III de Madrid, Leganés, Madrid, Spain

## References

[1] Toma T., Takizuka T., Kanou M., Taniguchi T., Koike Y. Dual full high definition 3D video real-time communication system. In: International Conference on Plastic Optical Fibers, ICPOF 2011, Bilbao, Spain, 2011, 475-479.

[2] Fischer U. H. P., Haupt M., Joncic M. Optical Transmission Systems Using Polymeric Fibers. In: Optoelectronics-Devices and Applications. InTech; 2011, 445-468.

[3] Koonen A. J., Tangdiongga E. Photonic Home Area Networks. Journal of Lightwave Technology 2014; 32(4) 591-604.

[4] Bilro L., Alberto N., Pinto J. L., Nogueira R. Optical Sensors Based on Plastic Fibers. Sensors 2012; 12 12184 – 12207.

[5] Ziemann O., Zamzow P. E., Daum W. POF Handbook: Optical Short Range Transmission Systems. Berlin: Springer Berlin Heidelberg; 2008.

[6] Okonkwo E. T. C. M., Yang H., Visani D., Loquai S., Kruglov R., Charbonnier B., Ouzzif M., Greiss I., Ziemann O., Gaudino R., Koonen A. M. J. Recent Results from the EU POF−PLUS Project: Multi−Gigabit Transmission Over 1 mm Core Diameter Plastic Optical Fibers. Journal of Lightwave Technology 2011; 29(2) 186-193.

[7] Li W., Khoe G., Boom H. V.D., Yabre G., De Waardt H., Koike Y., Yamazaki S., Nakamura K., Kawaharada Y. 2.5 Gbit/s Transmission over 200 m PPMA Graded Index Polymer Optical Fiber Using a 645 nm Narrow Spectrum Laser and a Silicon APD. Microwave and Optical Technology Letters 1999; 20(3) 163-166.

[8] Van Den Boom H. P. A., Li W., Van Bennekom P. K., Monroy I. T., Khoe G. D. IEEE Journal on Selected Topics in Quantum Electronics 2001; 7(3) 461-470.

[9] Niheii E., Ishigurett T., Taniott N., Koike Y. Present Prospect of Graded-lndex Plastic Optical Fiber in Telecommunication. IEICE Transactions on Electronics 1997; E80-C 117-121.

[10] Polley A., Ralph S. E. 100 m, 40 Gb/s Plastic optical fiber link. In: Optical Fiber communication/National Fiber Optic Engineers Conference, 2008, San Diego, 1-3.

[11] Vázquez C., Montero D. S. Multimode Graded-Index Optical Fibers for Next-Generation Broadband Access. In: Current Developments in Optical Fiber Technology. InTech; 2013.

[12] Jianjun Y., Dayou Q., Mingfang H., Zhensheng J., Chang G. K., Ting W. 16Gbit/ s radio OFDM signals over graded-index plastic optical fiber. In: 34th European Conference on Optical Communication, ECOC 2008, 2008, 1-2.

[13] Zeng J., Van den Boom H. P. A., Koonen A. M. J. Five-subcarrier multiplexed 64-QAM transmission over a 50-μm core diameter graded index perfluorinated polymer

pptical fiber. In: Optical Fiber Communication Conference/National Fiber Optic Engineers Conference, San Diego, California, 2008, OWB4.

[14] Lee S. C. J., Breyer F., Randel S., Gaudino R., Bosco G., Bluschke A., Matthews M., Rietzsch P., Steglich R., Van den Boom H. P. A., Koonen A. J. Discrete Multitone Modulation for Maximizing Transmission Rate in Step-Index Plastic Optical Fibers. Journal of Lightwave Technology 2009; 27(11) 1503-1513.

[15] Hejie Y., Lee S. C. J., Tangdiongga E., Okonkwo C., Van den Boom H. P. A., Breyer F., Randel S., Koonen A. J. 47.4 Gb/s Transmission Over 100 m Graded-Index Plastic Optical Fiber Based on Rate-Adaptive Discrete Multitone Modulation. Journal of Lightwave Technology 2010; 28(4) 352-359.

[16] Randel S., Lee S. C. J., Spinnler B., Breyer F., Rohde H., Walewski J., Koonen A. M. J., Kirstädter A. 1 Gbit/s transmission with 6.3 bit/s/Hz spectral efficiency in a 100m standard 1 mm step-index plastic optical fibre link using adaptive multiple sub-carrier modulation. In: Proceedings of the 32nd European Conference on Optical Communication, ECOC 2006, Cannes, France, 2006, Th4.4.1-1/2.

[17] Cardenas Lopez D. F., Nespola A., Camatel S., Abrate S., Gaudino R. 100 Mb/s Ethernet Transmission Over 275 m of Large Core Step Index Polymer Optical Fiber: Results From the POF-ALL European Project. Journal of Lightwave Technology 2009; 27(14) 2908-2915.

[18] Okonkwo C. M., Tangdiongga E., Yang H., Visani D., Loquai S., Kruglov R., Charbonnier B., Ouzzif M., Greiss I., Ziemann O., Gaudino R., Koonen A. J. Recent Results from the EU POF-PLUS Project: Multi-Gigabit Transmission Over 1 mm Core Diameter Plastic Optical Fibers. Journal of Lightwave Technology 2011; 29(2) 186-193.

[19] Ciordia O. Esteban C., Pardo C., Pérez de Aranda R. Commercial silicon for gigabit communication over SI-POF. In: International Conference on Plastic Optical Fibers, ICPOF 2013, Búzios, Brasil, 2013, 109-116.

[20] Wei J. L., Geng L., Cunningham D. G., Penty R. V., White I. H. Gigabit NRZ, CAP and Optical OFDM Systems Over POF Links Using LEDs. Optics Express 2012; 20(20) 22284-22289.

[21] Ziemann O., Bartiv L. POF-WDM, the truth. In: International Conference on Plastic Optical Fibers, ICPOF 2011, Bilbao, Spain, 2011, 525-530.

[22] Jončić M., Haupt M., Fischer U. H. P. Four-channel CWDM system design for multi-Gbit/s data communication via SI-POF. In: Proceedings of SPIE 9007: Broadband Acces Communication Technologies VIII, San Francisco, United States, 2013, 90070J.

[23] Jončić M., Kruglov R., Haupt M., Caspary R., Vinogradov J., Fischer U. H. P. Four-Channel WDM Transmission Over 50 m SI-POF at 14.77 Gb/s Using DMT Modulation. IEEE Photonics Technology Letter 2014; 26(13) 1328-1331.

[24] Musa A. B. S., Kok A. A. M., Diemee M. B. J., Driessen A. Multimode arrayed waveguide grating-based demultiplexers for short-distance communication. In: IEEE Eurocon, 2003, 422-426.

[25] Ehsan A. A. Shaari S., Rahman M. K. A. Plastic Optical Fiber Coupler with High Index Contrast Waveguide Taper. Progress in Electromagnetics Research C, 2011; 20 125-138.

[26] Jončić M., Haupt M., Fischer U. H. P. Four-channel CWDM system design for multi-Gbit/s data communication via SI-POF. In: Proceedings of SPIE 9007: Broadband Acces Communication Technologies VIII, San Francisco, United States, 2013, 90070J-90070J-9.

[27] Lutz D., Haupt M., Fischer U. H. P. Demultiplexer for WDM over POF in prism-spectrometer configuration. In: Photonics and Microsystems, 2008 International Students and Young Scientists Workshop, 20-22 June 2008, Worclaw, Poland, 43-46.

[28] Jončić M., Haupt M., Fischer U. H. P. Investigation on spectral grids for VIS WDM applications over SI POF.In: Proceedings of the Photonische Netze, ITG-FB 241, 6-7 May 2013, Leipzig, Germany, 1-6.

[29] L. V. Bartkiv, Bobitski Y. V., Poisel H. Optical Demultiplexer Using a Holographic Concave Grating for POF-WDM Systems. Optica Applicata 2005; 35(1) 59-66.

[30] Haupt M., Fischer U. H. P. Multi-colored WDM over POF system for Triple-Play. In: Proceedings of SPIE 6992: Micro-Optis 2008, 699213-699213-10.

[31] Chandrasekhar S. Liquid Crystals. Cambridge University Press; 1992.

[32] Riza N. A., Yuan S. Low Optical Interchannel Crosstalk, Fast Switching Speed, Polarization Independent 2x2 Fiber Optic Switch Using Ferroelectric Liquid Crystals. Electronis Letters 1999; 34(17) 1341-1342.

[33] Pain F., Coquillé R., Vinouze B., Wolffer N., Gravey P. Comparison of Twisted and Parallel Nematic Liquid Crystal Polarisation Controllers. Application to a 4 × 4 Free Space Optical Switch at 1.5 μm. Optics Communications 1997; 139(4-6) 199-204.

[34] Vázquez C., Pena J. M. S., Aranda A. L. Broadband 1 x 2 Polymer Optical Fiber Switches Using Nematic Liquid Crystals. Optics Communications 2003; 224(1-3) 57-62.

[35] Sumriddetchkajorn S., Riza N. A., Sengupta D. K. Liquid Crystal-Based Self-Aligning 2×2 Wavelength Routing Module. Optical Engineering 2001; 40(8) 1521-1528.

[36] Pena J. M. S., Rodríguez I., Vázquez C., Pérez I., Otón J. M. Spatial Distribution of the Electric Field in Liquid Crystal Dispersions Devices by using a Finite-Element Method. Journal of Molecular Liquids 2003; 108(1-3) 107-117.

[37] Pena J. M. S., Vázquez C., Pérez I., Rodríguez I., Otón J. M. Electro-optic System for Online Light Transmission Control of Polymer-Dispersed Liquid Crystal Windows. Optical Engineering 2002; 41(7) 1608-1611.

[38] Zubia J., Durana G., Arrue J., Garces I. Design and Performance of Active Coupler for Plastic Optical Fibres. Electronics Letters 2002; 38(2) 65-67.

[39] Chanclou P., Vinouze B., Roy M., Cornu C. Optical Fibered Variable Attenuator Using Phase Shifting Polymer Dispersed Liquid Crystal. Optics Communications 2005; 248(1-3) 167-172.

[40] Lallana P. C., Vázquez C., Vinouze B., Heggarty K., Montero D. S. Multiplexer and Variable Optical Attenuator Based on PDLC for Polymer Optical Fiber Networks. Molecular Crystals and Liquid Crystals 2008; 502(1) 130-142.

[41] Chen R. H. Liquid Crystal Displays: Fundamental Physics and Technology. Hoboken: Wiley; 2011.

[42] Lallana P. C., Vázquez C., Pena J. M. S., Vergaz R. Reconfigurable Optical Multiplexer Based on Liquid Crystals for Polymer Optical Fiber Networks. Opto-Electronics Review 2006; 14(4) 311-318.

[43] Lallana P. C., Vázquez C., Vinouze B. Advanced multifunctional optical switch for multimode optical fiber networks," Optics Communications 2012; 285(12) 2802-2808.

[44] Jončić M., Haupt M., Fischer U. H. P. Standardization proposal for spectral grid for VIS WDM applications over SI-POF. In: Proceedings of POF Congress, Atlanta, 2012, 351-355.

[45] Ziemann O., Krauser J., Zamzow P. E., Daum W., POF Handbook: Optical Short Range Transmission Systems. Springer; 2008.

[46] Chua S. J., Li B. Optical Switches: Materials and Design. Woodhead Publishing in Materials; 2010.

[47] De Dobbelaere P., Falta K., Gloeckner S., Patra S. Digital MEMS for Optical Switching. IEEE Communications Magazine 2002; 40 (3) 88-95.

[48] Ramaswami. R., Sivarajan K. N., Sasaki G.H. Optical Networks: a practical perspective. Morgan Kaufmann; 2002.

[49] Sapriel J., Charissoux D., Voloshinov V., Molchanov V. Tunable Acoustooptic Filters and Equalizers for WDM Applications. Journal of Lightwave Technology 2002; 20 (5) 892-899.

[50] D'Alessandro A., Smith D. A., Baran J. E. Polarisation-Independent Low-Power Integrated acousto-optic tunable filter/switch using APE/Ti polarisation splitters on lithium niobate. Electronics Letters 1993; 29(20) 1767-1769.

[51] Sakuma K., Ogawa H., Fujita D., Hosoya H. Polymer Y-branching thermo-optic switch for optical fiber communication system. In: 8th Microoptics Conference, MOF'01, 2001, Osaka, Japan, 24-26.

[52] Leuthold J., Joyner C. H. Multimode Interference Couplers with Tunable Power Splitting Ratios. Journal of Lightwave Technology 2001; 19(5) 700.

[53] Almeida V. R., Barrios C. A., Panepucci R. R., Lipson M. All-Optical Control of Light on a Silicon Chip," Nature 2004; 431 1081-1084.

[54] Xiaohua M., Kuo G. S.Optical Switching Technology Comparison: Optical MEMS vs. Other Technologies. IEEE Communications Magazine 2003; 41(11) S16-S23.

[55] Krahenbuhl R., Howerton M. M., Dubinger J., Greenblatt A. S. Performance and Modeling of Advanced Ti:$LiNbO_3$ Digital Optical Switches. Journal of Lightwave Technology 2002; 20(1) 92-99.

[56] Nashimoto K., Moriyama H., Nakamura S., Watanabe M., Morikawa T., Osakabe E., Haga K. PLZT electro-optic waveguides and switches. In: Optical Fiber Communication Conference and Exhibit, 2001. OFC 2001, 2001, PD10-PD10.

[57] Agranat A. J. Electroholographic wavelength selective crossconnect. In: Nanostructures and Quantum Dots/WDM Components/VCSELs and Microcavaties/RF Photonics for CATV and HFC Systems, 1999 Digest of the LEOS Summer Topical Meetings, 1999, II61-II62.

[58] Domash L. H., Yong-Ming C., Haugsjaa P., Oren M. Electronically switchable waveguide Bragg gratings for WDM routing. In Vertical-Cavity Lasers, Technologies for a Global Information Infrastructure, WDM Components Technology, Advanced Semiconductor Lasers and Applications, Gallium Nitride Materials, Processing, and Devi, 1997, 34-35.

[59] Wagner R. E., Cheng J. Electrically Controlled Optical Switch for Multimode Fiber applications. Applied Optics 1980; 19(17) 2921-2925.

[60] Vázquez C., Pena J. M. S., Aranda A. L. Broadband 1x2 Polymer Optical Fiber Switches Using Nematic Liquid Crystals. Optics Communications 2003; 224(1-3) 57-62.

[61] Vázquez C. Pena J. M. P., Contreras P., Pontes M. A. J. Development of a 2x2 optical switch for plastic optical fiber using liquid crystal cells. In: Proceedings of SPIE 5840: Photonics Materials, Devices and Applications. 2005, 325-335.

[62] Pinzón P. J., Pérez I., Vázquez C., Pena J. M. S. 1 × 2 Optical Router With Control of Output Power Level Using Twisted Nematic Liquid Crystal Cells," Molecular Crystals and Liquid Crystals 2012; 553 (1) 36-43.

[63] Macdonald R., Chen L. P., Shi C. X., Faer B. Requirements of optical layer network restoration. In: Optical Fiber Communication Conference, 2000, Vol. 3 68-70.

[64] Song D. H., Kim J.-W., Kim K.-H., Rho S. J., Lee H., Kim H., Yoon T.-H. Ultrafast switching of randomly-aligned nematic liquid crystals," Optics Express, vol. 20, pp. 11659-11664, 2012/05/21 2012.

[65] Ha Y.-S., Kim H.-J., Park H.-G., Seo D.-S. Enhancement of Electro-Optic Properties in Liquid Crystal Devices Via Titanium Nanoparticle Doping. Optics Express 2012; 20 (6) 6448-6455.

[66] Borshch V., Shiyanovskii S. V., Lavrentovich O. D. Nanosecond response in nematic liquid crystals for ultrafast electro-optic devices. In: CIOMP-OSA Summer Session on Optical Engineering, Design and Manufacturing, Changchun, 2013, Tu8.

[67] Amosova L. P., Vasil'ev V. N., Ivanova N. L., Konshina E. A. Ways of Increasing the Response Rate of Electrically Controlled Optical Devices Based on Nematic Liquid Crystals. Journal of Optical Technology 2010; 77(2) 79-87.

[68] Yeh P., Gu C. Optics of Liquid Crystal Display. New York: John Wiley&Sons; 2010.

[69] Pinzón P. J., Pérez I., Vázquez C., Sánchez-Pena J. M. Broadband 1×2 Liquid Crystal Router with Low Thermal Dependence for Polymer Optical Fiber Networks. Optics Communications 2014; 333 281-287.

[70] Vázquez C., Pérez I., Contreras P., Vinouze B., Fracasso B. Liquid Crystal Optical Switches. In: Li B., Chua S. J. (ed), Ed. Optical switches: Materials and design. Cambridge: Woodhead Publishing Limited; 2010.

[71] Marom D. M., Neilson D. T., Greywall D. S., Chien-Shing P., Basavanhally N. R., Aksyuk V. A., Lopez D. O., Pardo F., Simon M. E., Low Y., Kolodner P., Bolle C. A. Wavelength-Selective 1 x K Switches Using Free-Space Optics and MEMS Micromirrors: Theory, Design, and Implementation. Journal of Lightwave Technology 2005; 23(4) 1620-1630.

[72] Suzuki K., Mizuno T., Oguma M., Shibata T., Takahashi H., Hibino Y., Himeno A. Low Loss Fully Reconfigurable Wavelength-Selective Optical 1 x N Switch Based on Transversal Filter Configuration Using Silica-Based Planar Lightwave Circuit. IEEE Photonics Technology Letters 2004; 16(6) 1480-1482.

[73] Vázquez C., Contreras P., Montalvo J., Sánchez Pena J. M., d'Alessandro A., Donisi D. Switches and tunable filters based on ring resonators and liquid crystals. In: Proceedings of SPIE 6593: Photonics Materials, Devices and Applications 2007, 65931F-65931F-10.

[74] Pinzón P. J., Pérez I., Vázquez C., Sánchez Pena J. M. Reconfigurable 1 x 2 Wavelength Selective Switch Using High Birefringence Nematic Liquid Crystals. Applied Optics 2012; 51(25) 5960-5965.

[75] Pinzon P. J., Vazquez C., Perez I., Sanchez Pena J. M. Synthesis of Asymmetric Flat-Top Birefringent Interleaver Based on Digital Filter Design and Genetic Algorithm. Journal of Photonics 2013; 5(1) 7100113-7100113.

[76] Michael S. The Sun: an Introduction. Springer-verlag Co.; 2004.

[77] Montalvo J., Frazão O., Santos J., Vázquez C., Baptista J. Radio-Frequency Self-Referencing Technique With Enhanced Sensitivity for Coarse WDM Fiber Optic Intensity Sensors. Journal of Lightwave Technology 2009; 27(5) 475-482.

[78] Montero D. S., Vázquez C., Baptista J. M., Santos J. L., Montalvo J. Coarse WDM Networking of Self-Referenced Fiber-Optic Intensity Sensors with Reconfigurable Characteristics. Optics Express 2010; 18(5) 4396-4410.

[79] Othonos A., Kalli K. Fiber Bragg gratings: Fundamentals and Applications in Telecommunications and Sensing. Boston&London: Artech House; 1999.

[80] Xiong Z., Peng G. D., Wu B., Chu P. L. Highly Tunable Bragg Gratings in Single-Mode Polymer Optical Fibers. Photonics Technology Letters 1999; 11(3) 352-354.

[81] Dobb H., Webb D. J., Kalli K., Argyros A., Large M. C., van Eijkelenborg M. A. Continuous Wave Ultraviolet Light-Induced Fiber Bragg Gratings in Few- and Single-Mode Microstructured Polymer Optical Fibers. Optics Letters 2005; 30(24) 3296-3298.

[82] Roriz P., Ramos A., Santos J., Simões J. Fiber Optic Intensity-Modulated Sensors: a Review in Biomechanics. Photonic Sensors 2012; 2(4) 315-33.

[83] Mishra V., Singh N., Tiwari U., Kapur P. Fiber Grating Sensors in Medicine: Current and Emerging Applications. Sensors and Actuators A: Physical 2011; 167(2) 279-290.

[84] Berghmans F., Geernaert T., Sulejmani S., Thienpont H., Van Steenberge G., Van Hoe B., Dubruel P., Urbanczyk W., Mergo P., Webb D. J., Kalli K., Van Roosbroeck J., Sugden K. Photonic crystal fiber Bragg grating based sensors: opportunities for applications in healthcare. In: Popp J., Matthews D., Tian J., Yang C. (eds) Optical Sensors and Biophotonics, of Proceedings of SPIE 8311: Asia Communications and Photonics Conference and Exhibition, 2011, 831102-831102-10.

[85] Montalvo J., Frazao O., Santos J. L., Vazquez C., Baptista J. M. Radio-Frequency Self-Referencing Technique With Enhanced Sensitivity for Coarse WDM Fiber Optic Intensity Sensors. Journal of Lightwave Technology 2009; 27(5) 475-482.

[86] Montero D. S., Tapetado A., Webb D.J., Vázquez C. Self-Referenced Optical Intensity Sensor Network Using POFBGs for Biomedical Applications. Sensors 2014; p. in press.

[87] Vázquez C., Montero D.S., J. Zubia. Short-range transmission capacity analisys over PF GIPOF. In: International Conference on Plastic Optical Fibers (ICPOF), Atlanta, USA, 2012.

[88] Montero D. S., Vázquez C. Analysis of the Electric Field Propagation Method: Theoretical Model Applied to Perfluorinated Graded-Index Polymer Optical Fiber Links. Optics Letters 2011; 36(20) 4116-4118.

[89] Lethien C., Loyez C., Vilcot J.-P., Rolland N., Rolland P. A. Potential of the Polymer Optical Fibers Deployed in a 10Gbps Small Office/Home Office Network. Optics Express 2008; 16(15) 11266-11274.

[90] Lethien C., Loyez C., Vilcot J. P., Rolland N., Rolland P. Exploit the Bandwidth Capacities of the Perfluorinated Graded Index Polymer Optical Fiber for Multi-Services Distribution. Polymers 2011; 3(3) 1006-1028.

[91] Montero D. S., Vázquez C. Multimode Graded-Index Optical Fibers for Next-Generation Broadband Access. In: Harum S. W., Arof H. (ed) Current Developments in Optical Fiber Technology. InTech; 2013.

[92] Chow P. S., Cioffi J. M., Bingham J. A. C. A Practical Discrete Multitone Transceiver Loading Algorithm for Data Transmission over Spectrally Shaped Channels. IEEE Transactions on Communications 1995; 43 773-775.

[93] Bartkiv L., Poisel H., Bobitski Y. Wavelength Demultiplexer with Concave Grating for GI-POF systems. Optica Applicata 2005; 35.

[94] Van den Boom H. P. A., Li W., Khoe G. D. CWDM technology for polymer optical fiber networks. In: Proceedings of the 5th annual symposium of the IEEE/LEOS Benelux Chapter Netherlands, 2000, 13-16.

[95] Shi Y., Okonkwo C., Visani D., Tangdiongga E., Koonen T. Distribution of Broadband Services Over 1-mm Core Diameter Plastic Optical Fiber for Point-to-Multipoint In-Home Networks. Journal of Lightwave Technology 2013; 31(6) 874-881.